Evaluating the capability of regional-scale air quality models to capture the vertical distribution of pollutants

*Efisio Solazzo(1), Roberto Bianconi(2), Guido Pirovano(3), Michael D. Moran(4), Robert Vautard(5), Christian Hogrefe(6), K. Wyat Appel (6), Volker Matthias(7), Paola Grossi(2), Bertrand Bessagnet(9), Jørgen Brandt(8), Charles Chemel(12,13), Jesper H. Christensen(8), Renate Forkel (16), Xavier V. Francis(13), Ayoe B. Hansen (8), Stuart McKeen (18), Uarporn Nopmongcol (14), Marje Prank (11), Karine N. Sartelet(10), Arjo Segers (15), Jeremy D. Silver(8), Greg Yarwood (14), Johannes Werhahn (16), Junhua Zhang (4), S.T. Rao(6), Stefano Galmarini(1)**

(1) European Commission, Joint Research Centre, Institute for Environment and Sustainability, ISPRA, Italy
(2) Enviroware srl, Concorezzo (MB), Italy
(3) Ricerca sul Sistema Energetico (RSE SpA), Milano, Italy
(4) Air Quality Research Division, Science and Technology Branch, Environment Canada, Toronto, Canada
(5) IPSL/LSCE Laboratoire CEA/CNRS/UVSQ
(6) Atmospheric Modelling and Analysis Division, Environmental Protection Agency, NC, USA
(7) Institute of Coastal Research, Helmholtz-Zentrum Geesthacht, Geeshacht, Germany
(8) Department of Environmental Science, Aarhus University, Frederiksborgvej 399, 4000 Roskilde, Denmark
(9) Ineris, Parc Technologique Halatte, France
(10) CEREA, Joint Laboratory Ecole des Ponts ParisTech/ EDF R & D, Université Paris-Est, France
(11) Finnish Meteorological Institute, Helsinki, Finland
(12)National Centre for Atmospheric Science (NCAS), University of Hertfordshire, Hatfield, UK
(13)Centre for Atmospheric & Instrumentation Research (CAIR), University of Hertfordshire, Hatfield, UK
(14) ENVIRON International Corporation, 773 San Marin Drive, Suite 2115, Novato, CA 94998, USA
(15) Netherlands Organisation for Applied Scientific Research (TNO), Utrecht, The Netherlands
(16)Karlsruhe Institute of Technology, IMK-IFU, Garmisch-Partenkirchen, Germany
(18) CIRES/University of Colorado, and NOAA/ESRL/CSD, 325 Broadway, Boulder, CO, USA

*Author for correspondence: stefano.galmarini@jrc.ec.europa.eu

Abstract

This study is conducted in the framework of the Air Quality Model Evaluation International Initiative (AQMEII) and is aimed at the operational evaluation of an ensemble of twelve regional-scale chemical transport models used to predict air quality over the North American (NA) and European (EU) continents for 2006. The modelled concentration of ozone and CO, along with the meteorological fields of wind speed (WS) and direction (WD), temperature, and relative humidity (RH) are compared against high-quality in-flight measurements collected by instrumented commercial aircraft as part of the Measurements of OZone, water vapour, carbon monoxide and nitrogen oxides by Airbus In-service airCraft (MOZAIC) programme. The evaluation is carried out for five model domains positioned around four major airports in NA (Portland, Philadelphia, Atlanta, and Dallas) and one in Europe (Frankfurt), from the surface to 8.5 km. We compare mean vertical profiles of modelled and measured variables for all airports to compute error and variability statistics, perform analysis of altitudinal error correlation, and examine the seasonal error distribution for ozone, which also

includes an estimation of the bias introduced by the lateral boundary conditions (BCs). In general, the results indicate that model performance is highly dependent on the variable, location, season, and height (e.g., surface, PBL or free troposphere) being analysed. While model performance for temperature is satisfactory at all sites (correlation coefficient in excess of 0.90 and fractional bias ≤ 0.01K), WS is not replicated as well within the PBL (exhibiting a positive bias in the first 100 m and also underestimating observed variability), while above 1000 m, the model performance improves (correlation coefficient often above 0.9). The WD at NA airports is found to be biased in the PBL, primarily due to an overestimation of westerly winds. RH is modelled well within the PBL, but in the free troposphere large discrepancies among models are observed, especially in EU. CO mixing ratios show the largest range of modelled-to-observed standard deviations of all the examined species at all heights and for all airports. Correlation coefficients for CO are typically below 0.6 for all sites and heights, and large errors are present at all heights, particularly in the first 250 m. Model performance for ozone in the PBL is generally good, with both bias and error within 20%. Profiles of ozone mixing ratios depend strongly on surface processes, revealed by the sharp gradient in the first 2 km (10 to 20 ppb/km). Modelled ozone in winter is biased low at all locations in the NA, primarily due to an underestimation of ozone from the BCs. Most of the model error in the PBL is due to surface processes (emissions, transport, photochemistry), while errors originating aloft appear to have relatively limited impact on model performance at the surface. Suggestions for future work include interpretation of the model-to-model variability and common sources of model bias, and linking CO and ozone bias to the bias in the meteorological fields. Based on the results from this study, we suggest that in-depth, process-oriented and diagnostic investigations be carried out next.

Keywords: AQMEII, model evaluation, MOZAIC, ozone, ozonesonde

1. Introduction

Air quality (AQ) model evaluation studies are typically focused on the assessment of performance with respect to surface measurements since the primary goal of AQ models is to simulate the fate of pollutants to which humans, and the biosphere as a whole, are directly exposed, and also because regulatory limits are imposed at ground level only. Examples of model evaluation studies using only ground-level measurements are numerous (e.g., Van Loon et al., 2007; Vautard et al., 2009 and 2012; Solazzo et al., 2012a,b; Appel et al., 2007,2008 and 2012). Evaluation of AQ models in the troposphere, from the ground to well above the planetary boundary layer (PBL), has been performed much less frequently than ground level only studies. Some specific experimental (e.g., Cros et al., 2004, Drobinski et al., 2007; Yu et al., 2007 and 2010; Wei et al., 2011) or case studies (e.g. Emeis et al., 2011, Matthias et al., 2012) using upper-level measurements do exist, but comprehensive tropospheric evaluation and model inter-comparisons over long time periods are missing.

The development of policies designed to control and reduce air pollution requires an accurate knowledge about the sensitivity of atmospheric concentration to changes in anthropogenic emissions. This sensitivity is modulated by a number of factors, including atmospheric conditions and their variability, the state of the land surface, deposition, and concentrations of long-range transported pollutants, and primary emissions that produce a chemical environment in which secondary air pollutants develop. All of these factors influence, and are influenced by, the three-dimensional spatial distribution of pollutants and the variability of the latter over time. Accurate simulation of the

troposphere is crucial from the perspective of emission control, and requires testing the capability of models to represent the vertical distribution of pollutants, the exchanges between the PBL and the free troposphere, and the horizontal fluxes between continental domains (Jonson et al., 2010; Gilge et al., 2010; Brunner et al., 2005). In addition, the pivotal role of the meteorological forcing in determining the fate of pollutant species cannot be underestimated as errors in meteorology are inherited by AQ models, thereby producing errors in model-predicted pollutant concentrations, which can result in compounding or compensating errors. This is particularly true for long-lived species, whose concentrations are determined by the history of air parcels over long time periods during which meteorological errors may accumulate (e.g., Brunner et al., 2003; Blond and Vautard, 2004). Recent reports by the US National Research Council and the United Nations Task Force on Hemispheric Transport of Air Pollution (HTAP) (Szykman et al., 2012 and references therein) have urged the need for quality upper-air observational data to support model development and help address model deficiencies in the troposphere.

Examples of ensemble model evaluation in the troposphere do exist for global chemical transport models. Stevenson et al. (2006) analysed 26 global model simulations evaluated against ozonesonde profiles for the year 2000. The study suggested that the primary sources of ozone in the troposphere are chemical production and influx from the stratosphere (the latter was estimated as being about a tenth of the production term), and that removal is determined by chemical transformation and dry deposition. Furthermore, the authors showed that the ensemble mean of model results for ozone typically ranges within one standard deviation of the measurements over the entire depth of the troposphere. However, several significant discrepancies were detected, depending on location and season as for example over-prediction throughout the northern tropics and overestimation of winter ozone at 30°-90° N. A further example of ensemble modelling of tropospheric ozone is reported by Jonson et al. (2010), who compared the ensemble mean from 12 global scale models against ozonesonde profiles in the framework of HTAP for the year 2001. The ensemble mean bias of models was found to be smaller in winter and fall, with large day-to-day variability among the models. Generally, model performances were higher at locations closer to major sources than in remote locations, with the best scores detected for Goose Bay (east NA) while the poorest for the Arctic stations. The modeled standard deviation was found to be low in the upper troposphere compared to the ozonesondes at all sites. The authors attributed this latter behaviour of the models to the difficulties to resolve plumes at remote stations due to the coarse grid spacing (ranging from 1° to 4°) of global models. Most recently, Zyryanov et al. (2012) conducted a comparative three-dimensional analysis of six regional AQ models over Europe using MOZAIC (Measurements of OZone, water vapour, carbon monoxide and nitrogen oxides by Airbus In-service airCraft) observations, focusing on ozone during the summer months of 2008. The authors found that a large model-to-model variability existed in the upper troposphere, between 8 and 10km height. Although a definitive reason for such variability could not be identified, the authors suggested that the differences in the model transport schemes, horizontal and vertical grid spacing, treatment of the top BCs, and the way that vertical velocity is computed (diagnostically or as output of the meteorological model) could be at least partially responsible for the variability between the models. Data from MOZAIC were also used by Elguindi et al. (2010) to evaluate the performance of four chemical transport models against vertical profiles of CO for the year 2004. In addition, there are also a number of case studies where individual

regional-scale models are compared to three dimensional concentration data collected during intensive measurement campaigns (e.g. Fisher et al., 2006; Tulet et al., 2002; Boynard et al., 2011).

However, none of the aforementioned studies is devoted to systematically evaluating an ensemble of regional-scale AQ models in the troposphere for extended periods and for several fields. Recently, a large effort within the air-quality community was established with the aim of evaluating many different regional-scale AQ modelling systems (Rao and Galmarini, 2011). The Air Quality Modelling Evaluation International Initiative (AQMEII) is the first consortium to provide a platform to evaluate the capability AQ models to simulate pollutant transport and transformation processes throughout the PBL and the free troposphere. The specific goal of AQMEII is to perform an initial set of model evaluations and inter-comparisons on existing regional AQ model systems in NA and EU. To accomplish this goal, model simulations were conducted for the year 2006 for North America (NA) and Europe (EU) model domains by independent modelling groups from both continents, using state-of-the-science regional AQ modelling systems. Previous AQMEII analyses had focused on the evaluation of ensemble of AQ models at surface, using observational data provided by the regulatory ground-based networks in EU and NA for ozone, particulate matter, and meteorological fields (Solazzo et al., 2012a,b; Vautard et al., 2012) for the year of 2006.

In the present study we extend the evaluation analyses to include the vertical component. We operate in the framework of the four-components of model evaluation proposed by Dennis et al. (2010), which is the main pillar of AQMEII (Rao and Galmarini, 2011). The primary goal of the analysis presented here is the operational evaluation of models in the troposphere, attempting to identify and quantify discrepancies between the models and measurements, and then suggesting hypotheses that should be investigated in detail as part of subsequent diagnostic evaluations (Rao et al., 2011). This study is therefore not intended to be an in-depth diagnostic analysis but rather an illustration the potential of using upper-air measurements for regional-scale model evaluation, by introducing various approaches, metrics, and methods to analyse the complex upper-air dataset, and set the stage for future work. Particular emphasis is put on ozone due to its importance on human-health and climate, and also because a complementary model evaluation for ground-level ozone is available for AQMEII (Solazzo et al., 2012a)

2. Processing of four-dimensional observational data in the context of AQMEII

In this study we make use of the observational data for the year 2006 gathered by the MOZAIC programme in NA and EU airports. Ozonesonde measurements are also used for further comparison in special cases.

The MOZAIC project started in 1993 as a joint effort of European scientists, aircraft manufacturers and airlines to develop a better understanding of the natural and anthropogenic variability of the chemical composition of the atmosphere. The collection of chemical species and of meteorological drivers includes a large number of vertical profiles measured at several airports worldwide during the landing and take-off phases with a rate of data collection of 4 seconds, corresponding to approximately 50–100m in the vertical. The limit of detection is rather low (2 ppbv for ozone) with an error of only 2%, thus making the MOZAIC dataset very accurate (Marenco et al., 1998; Thouret et al.,

1998). Permission to access to the MOZAIC dataset for the reference year of 2006 was granted to the AQMEII community, allowing analysis of over 2000 vertical profiles measured by instrumented commercial aircraft landing and taking-off from 12 selected airports in North America (i.e. Portland, Vancouver, Atlanta, Dallas, Charlotte, Boston, Chicago, Montreal, New York, Philadelphia, Toronto, and Washington D.C.) and three in Europe (i.e. Frankfurt, Munich, and Vienna). These profiles contain the following species and meteorological fields: ozone, CO, temperature, relative humidity (RH), wind speed (WS) and direction (WD).

For the purposes of AQMEII, the "MOZAIC domains" that contained all the trajectories up to the altitude of approximately 13km over the year of 2006 are identified around each airport. This was particularly useful in the case, for example, of the Northeast US where trajectories of aircrafts landing in Washington D.C. passed over New York airports too. Similarly, in EU, all the trajectories relating to Vienna also passed over Munich and Frankfurt. After we identified the MOZAIC domains, thirteen vertical levels above the ground were selected at 0, 100, 250, 500, 750, 1000, 2000, 3000, 4000, 5000, 6000, 7500, and 8500 m to be relevant to the analysis of the model results.

MOZAIC data were gathered during take-off and landing phases, with larger occurrences of early-to-mid-afternoon (corresponding to landings in NA) and mid-to-late afternoon (corresponding to take-offs in NA) local time flights, approximately 70% of which occurred during spring and summer. Table 1 gives the list of airports within each simulation domain and the number of MOZAIC flights associated with each airport during 2006. To simplify the analysis, the airport with the largest number of flights is selected and used for the analysis. In total five areas (four in NA and one in EU) are identified to be analysed in this study. The Portland and Philadelphia airports are selected to represent the west and east coasts of NA, respectively, while the Dallas and Atlanta airports represent the two other areas of NA. Frankfurt (with over 1200 hourly flights) had the best yearly coverage and represents the central EU area. The location of the airports and flight areas are shown in Figure 1.

In addition to the MOZAIC measurements, ozonesonde data were extracted from the World Meteorological Organisation (WMO) World Ozone and Ultraviolet Radiation Data Centre in Toronto (Canada) and made available to the AQMEII community. These measurements report vertical profiles of ozone partial pressure at several vertical pressure levels. Further details on these data are given in (Schere et al., 2012).

2.1 Pairing models and observational data

The groups participating in AQMEII were requested to deliver their model results for the species, time, location, and altitude for which observational data were available. The model data corresponding to the three-dimensional grid enclosing the MOZAIC trajectories at the aforementioned thirteen altitudes were subsequently delivered to European Commission's Joint Research Centre in Ispra (Italy) by each modelling group, with a common horizontal grid resolution for the whole period of 2006 with one-hour time resolution. Hosting the data is the ENSEMBLE system (Galmarini et al., 2004; 2012), a web-interfaced data hub allowing model and observed data to be harmonized and paired in time and space so to facilitate the model evaluation. Once a specific airport, date, and flight are selected, the ENSEMBLE system automatically extracts the model data from the domain volume and couples them with the MOZAIC profiles in space and time. Since measurements

and model results are stored in ENSEMBLE at the same heights, the trajectory analysis module in ENSEMBLE works by looping through the measurement points along each three-dimensional trajectory.

3. Participating models

The participating research groups and modelling systems used are reported in Table 2. In total, four to five (depending on the variable) groups delivered data to compare against the MOZAIC profiles for NA, whereas data from eight to nine groups were available for EU.

The emissions and chemical BCs used by the various AQMEII groups are summarised in Table 2. AQMEII provided a set of reference time-varying gridded emissions (referred to as the "standard" emissions) for each continent. These inventories have been extensively discussed in other AQMEII publications (Pouliot et al., 2012; Solazzo et al., 2012a,b). Although the standard emissions were used by the vast majority of the participating AQMEII groups, there still were a number of degrees of freedom (e.g., fire emissions or biogenic emissions) which were chosen by each group independently. Model results generated with other emissions inventories were also submitted. AQMEII also provided a set of time-dependent chemical concentrations at the lateral boundaries of the EU and NA domains, referred to as the "standard" BCs, extracted from the Global and regional Earth-system Monitoring using Satellite and in-situ data (GEMS) re-analysis product provided by the European Centre for Medium-range Weather Forecast (ECMWF) (Schere et al., 2012). These standard BCs were used by the majority of the modelling groups, although other BCs for ozone were also used, which were based on satellite measurements assimilated within the Integrated Forecast System (IFS). Models were driven by different meteorological simulations, which were described and evaluated in Vautard et al. (2012). Details on the model configurations are given in Table 2.

3.1 Participating models and settings

3.1.1 WRF-CMAQ

The model configurations used by the US EPA and the University of Herthfordshire are similar for NA and EU, with both simulations utilizing the Community Multiscale Air Quality (CMAQ) model version 4.7.1 (Byun and Schere, 2006; Foley et al., 2010). The NA simulation uses 34 vertical layers and 12 km horizontal grid spacing covering the CONUS, southern Canada and northern Mexico, while the EU simulation uses 34 vertical layers and 18 km horizontal grid spacing covering most of EU. Other model options employed that are common to both simulations include the CB05 chemical mechanism (Yarwood et al., 2005) with chlorine chemistry extensions, the AERO5 aerosol module (Carlton et al., 2010), and the Asymmetric Convective Model 2 (ACM2) vertical mixing scheme (Pleim, 2007a,b). Additional details regarding the WRF-CMAQ simulations for AQMEII can be found in Appel et al. (2012) and references therein.

3.1.2 ECMWF-SILAM

The SILAM (Sofiev et al., 2006) model uses a transport algorithm based on the non-diffusive Eulerian advection scheme of Galperin (1999, 2000) and the adaptive vertical diffusion algorithm of Sofiev

(2002). The use of sub-grid variables in these schemes allows the model to be used with thick vertical layers. A detailed description can be found in Sofiev et al. (2008). SILAM includes a meteorological pre-processor for diagnosing the basic features of the PBL and the free troposphere (e.g., diffusivities) from the meteorological fields provided by meteorological models (Sofiev et al., 2010). Only horizontal wind components are taken from the meteorological input and the vertical component is computed from the continuity equation. SILAM is a terrain-following height coordinates models and for the AQMEII simulations the model consisted of 9 layers up to approximately 10 km.

3.1.3 MM5-DEHM

The Danish Eulerian Hemispheric Model (DEHM) (Christensen, 1997; Frohn et al., 2002; Brandt et al., 2012) is a 3D long-range atmospheric chemistry-transport model with a horizontal domain covering the Northern Hemisphere with 150km horizontal grid spacing. For AQMEII, the model includes two two-way nested domains, one covering EU and one covering NA, and both with 50 km horizontal grid spacing. The vertical grid is defined using the σ-coordinate system, with 29 vertical layers extending up to 100 hPa. The horizontal advection is solved numerically using the higher-order Accurate Space Derivatives scheme, applied in combination with a Forester filter (Forester, 1977). The vertical advection, as well as the dispersion sub-models, is solved using a finite elements scheme for the spatial discretisation. For the temporal integration of the dispersion, the method is applied and the temporal integration of the three dimensional advection is carried out using a Taylor series expansion to third order. The three dimensional wind fields are derived from the meteorological MM5 model, corrected in DEHM to ensure mass conservation. DEHM also includes a module for diagnostically calculating the vertical wind. For ozone, the initial and BCs (both lateral and top) are based on ozonesonde measurements, interpolated to global monthly three dimensional values with a grid spacing of 4^{o} x 5^{o} (Logan, 1999). A thorough description of DEHM and model setup for AQMEII is given in Brandt et al. (2012).

3.1.4 MM5-CHIMERE

The CHIMERE model (Bessagnet et al., 2004; Schmidt et al., 2001) applied over EU uses a 0.25° (~25km) horizontal grid spacing nine vertical layers expressed in a hybrid sigma-pressure coordinate system between surface and the 500 hPa pressure level. The first near-surface layer height was 20 m. All meteorological fields are interpolated from driver meteorology (MM5), with the vertical velocity recalculated to preserve mass balance. Turbulence in the PBL is represented using a diffusivity coefficient following the parameterization of Troen and Mahrt (1986) without the counter-gradient term. The second-order Van Leer scheme (van Leer, 1979) is used for the horizontal transport, and horizontal diffusion is neglected. Top BCs are obtained from the GEMS re-analysis at 3-hour interval and interpolated in three dimensions. The depth of the PBL is taken directly from MM5. Full model documentation is available at http://euler.lmd.polytechnique.fr/chimere

3.1.5 ECMWF- LOTOS-EUROS

The LOTOS-EUROS model (Schaap et al., 2008) simulated pollutant concentrations over EU at a regular horizontal grid spacing of approximately 25 km. In the vertical, the model is defined on four layers: a 25m surface layer, the PBL, and 2 residual layers with a top at 3.5km (or higher in mountainous areas). The height of the PBL, as well as the other meteorological input, is taken from ECMWF meteorological fields (short range forecasts over 0-12 hour at 3-hour interval). Advection of

tracers is implemented in all three dimensions following Walcek (2000), where vertical mass fluxes are derived from the mass balance. Vertical mixing is primarily determined by the growth of the second model layer following the rise of the PBL during the day, which leads to mixing of concentrations from the residual layer to the lower layer. Additional vertical mixing is implemented following standard K-diffusion (Louis, 1979). In the horizontal direction, no explicit diffusivity was added, apart from the numerical diffusion implied by the advection on a discrete grid.

3.1.6 MM5-Polyphemus

The Polyphemus AQ modelling platform is used with the Polair3D Eulerian chemistry transport model (Sartelet et al. 2012). Over EU, the horizontal resolution is 0.25° (~25km). Polyphemus used terrain-following height coordinates with nine vertical layers ranging from 20 to 9000m for the AQMEII simulation. The reactive-transport equations are solved using operator splitting (sequence: advection, diffusion, chemistry and aerosol). The advection scheme is a direct space-time third-order scheme with a Koren flux-limiter. Diffusion and chemistry are solved with a second-order Rosenbrock method. The vertical eddy-diffusion coefficient is parameterized following Louis (1979), except in the unstable convective PBL where the coefficients are calculated using the parameterization of Troen and Mahrt (1986). The horizontal diffusion coefficient is constant and equal to 10000 m^2 s^{-1}. In the AQMEII simulation, meteorological fields are interpolated from MM5, except for the eddy-diffusion coefficient and the vertical velocity, which are derived from the continuity equation.

3.1.7 GEM-AURAMS

The AURAMS model (Gong et al., 2006; Smyth et al., 2009) applied for AQMEII on the NA domain uses a secant polar-stereographic map projection true at 60°N, with 45km horizontal grid spacing. In the vertical, 29 layers are used with a terrain-following modified-Gal-Chen vertical coordinate and relatively thin layers near the surface (the first five layers were located at 0, 14, 55, 120, and 196 m) increasing monotonically in thickness to a model top at ~22km. Horizontal and vertical advection are both calculated using a semi-Lagrangian advection scheme (e.g., Pudykiewicz et al., 1997) with wind components provided by the GEM meteorological model (Côté et al., 1998a,b; Mailhot et al., 2006). The vertical diffusion operator is solved using an implicit first-order Laasonen scheme, where the vertical eddy-diffusion coefficient is parameterized in GEM using a turbulence kinetic energy scheme (Benoit et al., 1989; Belair et al., 1999). Horizontal diffusion is neglected. Model output is only saved for the first 20 layers, so vertical profiles are only available for the AURAMS model up to 5km.

3.1.8 WRF-WRF/Chem

The only model with atmospheric chemistry coupled online with the meteorology applied within this study is the community WRF/Chem mode (Grell et al., 2005). The two instances of WRF/Chem applied for EU are the same in all aspects except that only one (referred to as WRF/Chem1) includes feedback of the direct and indirect aerosol radiative effects to meteorology. The other instance is referred to as WRF/Chem2. Both simulations are set up with a horizontal grid spacing of 22.5km, 36 vertical layers, and identical physics and chemistry options as described by Forkel et al (2012). Gas-phase/aerosol chemistry and non-hydrostatic physics within WRF/Chem are tightly coupled, with 5th-order horizontal, 3rd-order vertical, and a 3rd-order Runge–Kutta time integration scheme (Skamarock et al., 2008). YSU PBL physics (Hong et al., 2006) are used for vertical mixing within the PBL. BCss for all species are from the default WRF/Chem configuration, which are designed to be representative for

clean, mid-latitude Pacific Ocean conditions. In spite of major differences in simulated solar radiation for cloudy conditions only small differences between the two model versions were found, since simulated temperature, humidity, and wind are nudged to the driving global analysis above the PBL for the simulations discussed here (Forkel et al, 2012).

3.1.9 Cosmo-CLM-CMAQ

At the HZG Institute, the CMAQ model is setup using 24 km horizontal grid and 30 vertical layers for both continents. Eleven of the 30 layers are below 1000 m, with the lowest layer top at approximately 36 m. Version 4.6 of the CMAQ (Matthias et al, 2010, Aulinger et al., 2011) model was used for the EU domain, while version 4.7.1 of the model was used for NA (the same version as the other CMAQ participants). Horizontal and vertical advection schemes in CMAQ use a modification of the piecewise parabolic method (PPM; Colella and Woodward, 1984). At each grid cell, a vertical velocity component is derived from the horizontal advection that satisfies the continuity equation using the density from driving meteorological model. In CMAQ 4.7.1, this scheme is further modified by adjusting the vertical velocities by the ratio of upwind fluxes to PPM calculated fluxes. Vertical diffusion is based on the asymmetric convective model (ACM; Pleim and Chang, 1992). In both CMAQ 4.6 and 4.7.1, version 2 of the ACM (ACM2; Pleim, 2007, 2007a) is implemented. The minimum value for the eddy diffusivity depends on the land-use of the individual grid cells and varies between 0.5 m^2 s^{-1} in grid cells with no urban areas and 2 m^2 s^{-1} in grid cells that contain only urban area. Zero flux BCss are used at the horizontal borders and at the top of the domain.

3.1.10 WRF/MM5-CAMx

Simulations for both the NA and EU continents uses CAMx version 5.21 (ENVIRON, 2010), with the CB05 chemical mechanism (Yarwood et al., 2005). The EU domain has 0.125° by 0.25° (~ 12km x 25km) latitude-longitude grid spacing and 23 vertical layers that follow WRF pressure levels between the surface and 100 hPa. The MM5 vertical domain has 32 vertical layers with a 30 m deep surface layer. CAMx employed fewer vertical layers (23) than MM5 to reduce the computational burden of the air quality simulations. The CAMx vertical layers exactly matched those used in MM5 for the lowest 14 layers (up to ~1800 m) and above this altitude were aggregates of several MM5 layers. The top CAMx layer placed at 12 km height was 3400 m deep.The NA domain has 12km horizontal grid spacing and 26 layers that follows MM5 pressure levels between the surface and 50 hPa. The BCs and emissions provided by AQMEII are used with the exception of biogenic emissions for EU which are estimated using MEGAN (Guenther et al., 2006). The CAMx vertical transport scheme is described by Emery et al. (2011) with vertical advection solved by a backward-Euler (time) hybrid centred/upstream (space) scheme and vertical diffusion solved using K-theory.

4. Model performance in the troposphere

4.1 Mean vertical profiles

Figure 2 presents the comparison of modelled versus observed seasonal averaged mean profiles of ozone and annual averaged mean profiles of CO, T, RH and WS. Observations are the grey symbols. While interpreting the results it should be kept in mind that a source of model underestimation may derive from the incommensurability of comparing point measurements over airports to grid cell model values (Elguindi et al., 2010).

All models show similar mean profiles of wind above the PBL and temperature from the ground to higher level and in agreement with the observed profiles, most likely due to the nudging techniques applied to these fields. The MM5-DEHM is the only model showing a positive bias for WS which increases with altitude at all sites, possibly due to the grid spacing, which is two to three times coarser than the other models. RH profiles have the lowest bias within the first ~2km, but significantly diverge above that height at all sites. It should be noted that in regions where the water vapour mixing ratio is very low (e.g., in the diverging zone), small differences in temperature can give rise to significant differences in RH. The RH peaks at 1000m at all airports, although with different magnitudes. The peak is generally well captured by the models at all airports, with the exception of Dallas, where the bias at 1000m ranges between 7 to 15%.

The observed annual mean profiles of CO peak at ground level and diminish monotonically with altitude. The rate of decay is faster in the first 1.5-2.5 km (dependant on the airport) due to enhanced mixing near the surface, and is smoother aloft. This feature is common to all sites. The value of the observed CO peak ranges between a minimum of 166 ppb at Dallas and a maximum of 250 ppb at Frankfurt, with the remaining airports all in the range of ~200 ppb. Being CO a directly emitted pollutant, its concentration is primarily determined by local emissions and BCs for CO. The modelled profiles of CO are significantly biased, most severely near the ground, with few exceptions. The modelled profiles of CO are significantly biased, typically with the largest bias near the ground, with few exceptions. While the DEHM model is biased low throughout the altitudinal range at all sites, the other models tend to have high biases near the ground, the exception being the CCLM-CMAQ model which performs the best in general, possibly due to a more effective vertical mixing scheme employed by the CCLM driver which with respect to WRF which drives the other instance of CMAQ.

Mean profiles of observed CO show a steep decrease in mixing ratio in the first 2 km, with an average gradient ranging between approximately -24 ppb/km (Dallas and Philadelphia) and -37 ppb/km (Atlanta), while Frankfurt is an outlier at 57 ppb/km. Between 2 and 8 km, the rate of decrease in CO mixing ratio considerably less, with a gradient of approximately 5-6 ppb/km at all airports. Averaged profiles of modelled CO show that ground-level mixing ratios can differ by up to a factor of 2, although differences are smaller above the PBL, but still significant, as discussed in detail with the aid of Taylor diagram in Section 4.2.4 (the large range of the horizontal axis in Figure 2 has the effect of clustering the observed and modelled profiles at any given altitude, thus deceptively reducing the bias). A possible reason for the difference might be related to the horizontal grid spacing of the AQ model (e.g. Brunner et al., 2003). As shown in Table 2, the DEHM model, which has the coarsest horizontal grid resolution, simulated the lowest mixing ratios, whereas the CAMx and CMAQ models, with much smaller horizontal grid spacing, simulated the highest mixing ratios. Another possible reason could be related to the influence of the chemical BCs to CO and ozone. At the NA airports that are closer to the boundaries (i.e. Portland and Philadelphia) the models that used GEMS BCs (i.e. CMAQ and CAMx) simulated CO mixing ratios that are closer to each other in magnitude than the DEHM and AURAMS models, which are driven by different BCs (model sensitivity to BCs is further discussed in Section 6).

The seasonal averaged ozone has the lowest mixing ratios in winter (all airports) and the typical maximum in spring and summer. The mean ozone mixing ratio increases with altitude in the first 1000 m, as near-ground depletion by deposition and titration reduce the ozone availability (e.g. Chevalier et al., 2007). The strong effect of surface processes on ozone is also evident by the strong gradient in the first 2 km of the troposphere, ranging on average between 10 to 20 ppb/km at all sites. Modelled ozone mixing ratio in winter is typically biased low at all locations, with the exception of the DEHM model (both NA and EU). The CCLM-CMAQ, MM5-CAMx, and SILAM for EU are all biased high above approximately 6 km throughout the year, likely due to inadequate representation of the tropopause in the model, which results in too much mixing between the high stratospheric ozone mixing ratios in the BCs and the troposphere in the model. Ozone within the PBL is generally overestimated in the summer (NA only), while in the fall the simulated mixing ratios are closer to the observed values, especially for Frankfurt. Layered ozone structures are most notable in summer months in the lowest levels close to the surface as result of the photochemistry and thermal mixing. At Portland, by contrast, the observed ozone in JJA peaks at 3 km and is under estimated by all models. A relative minimum of RH at the same height (annual average), which corresponds to the plateau values (~45%) of RH above 3 km might indicate a downward intrusion of ozone from the upper troposphere (Tulet et al., 2002). The lack of seasonal variation of ozone for WRF/Chem in the upper air is due to the use of constant background values of ozone as BCs.

4.2 Operational statistics and variability

In this section, operational statistics are presented with the aid of Taylor diagrams (Taylor 2001), which simultaneously show error, standard deviation and Pearson Correlation Coefficient (PCC). In a Taylor diagram, the observed field is represented by a point at a distance from the origin along the abscissa that is equal to the variance. All other points on the plot area represent values for the simulated fields and are positioned such that the variance of the modelled fields is the radial distance from the origin, the correlation coefficient of the two fields is the cosine of the azimuthal angle (desired value: 1), and the RMSE is the distance to the observed point (desired value: 0). In practical terms, the closer a model point is to an observed point, the better the model performance.

To synthesise the discussion we present annually averaged statistics (Figures 3-6). At any given height, the number of paired observation-model data is the same as the number of MOZAIC flights for all of 2006 reported in Table 2. Because flight paths differ between ascents and descents and can also vary due to meteorological conditions, the horizontal spatial location of the various measurements for a given altitude will also vary, and computing a temporal average across all data points also implies computing a spatial average. The spatial coverage of the virtual “horizontal plane” containing the individual flight trajectories over which the spatial averaging is calculated depends on the height. While the z = 0 level has the spatial coverage of a point (having the airport’s coordinates), that of the z = 8.5 km level is much larger, containing all the trajectories (ascending and descending) to and from the airport. This aspect has an influence on the spread of the data, as we shall discuss next. Coefficients of variation (CoV), defined as the ratio between the standard deviation and the average of the annual distribution at any height, have been calculated in order to assess the model’s capability of reproducing the observed variability. For synthesis, CoVs are shown for Frankfurt only (Figure 7), but are discussed for all airports.

Performance for temperature is considered to be satisfactory for all models, at all domains for at least the first 5 km (PCC in excess of 0.90 and fractional bias ≤ 1%). For this reason, analysis for temperature is not shown.

4.2.1 Wind Speed

For all the airports all models show significant errors in the modelled WS, and poor correlation with the observed values in the first 100 m. Although the sign of the bias cannot be deduced from a Taylor diagram, further analysis (not shown) indicates that the models are biased high. Smaller errors (still positive bias) are also observed at 500 and 1000 m. Poor correlation and moderate to high error within the PBL are common to all models at all sites, thus indicating that the meteorological models are not reproducing WS in the PBL precisely, which is arguably the most important region of the atmosphere in relation to air quality processes. This result supports the findings by Vautard et al. (2012) for the ground-based measurements. The poor model performance in the first 100 m at all sites is also confirmed by the analysis of the CoV, with modelled values well below the observations. A feature emerging is the clustering of performance based on altitude rather than on modelling system. For heights below the PBL, all models show the same deficiencies, indicating that incorrect simulation of WS near the surface is a common problem. There may be several reasons for this. First, near-surface winds are sensitive to several driving factors other than the synoptic circulation, such as land cover and surface energy exchange processes which have been found to exhibit large model-to-model variability in global and regional models (see e.g. de Noblet-Ducoudré et al., 2012, Stegehuis et al., 2012). Second, unlike upper-air winds which are measured by rawinsondes and are incorporated in reanalysis products, surface winds are not used for producing reanalyses. Therefore, even with a strong nudging of the wind field to the reanalyses, a lower model skill is expected for surface winds as compared to upper-air winds. This is demonstrated by the improvement of model performance above 500 m. For all models at all sites, and more markedly at Portland and Philadelphia, PCC, error and variability improve constantly with height. In general, the best performance by all models is observed for $z \geq 3$ km, with PCC > 0.8 at all NA sites, with the exception of the WRF/Chem model (PCC~0.65 at z=3 km), and at Frankfurt.

4.2.2 Wind direction

Although of pivotal importance for the transport of the polluted air masses, evaluation of the modelled WD is often overlooked. In this section we summarise the results of evaluating the AQ models of Table 2 using observed WD data from ground to 8.5 km. To simplify the analysis we have binned the frequency counts of the occurrences of WD angle with 20° interval. Results are discussed in terms of normalised bias (modelled minus observed count, and divided by the observed count). In general, we find that the bias in the PBL for the Frankfurt airport is smaller and decreases faster with height with respect to the NA airports. For the NA airports, in general there is a large bias within the PBL which is most pronounced on the west coast (Portland), thus pointing to biased BCs for WD.

For the Portland airport, WRF-CMAQ and GEM show similar biases from 0 to 500 m: positive for north-west and negative for south-east (~ 100%). The other models are biased low in the eastern sector. From z = 500 m the bias becomes larger and all models show a clear tendency to overestimate

the occurrences of westerly and easterly winds. From approximately 1000 m height, the bias reduces and the models reproduce the frequency distribution of observed WD satisfactorily. On the east coast of NA (Philadelphia airport), isolated cases of large bias are detected at 500 m and at 4 km height, where the two WRF models are biased high in the north and south sectors, respectively. For the inland airports of Atlanta and Dallas some occurrences of severe bias are detected. For the Atlanta airport, all models are biased high in the west and north-west directions (50%) in the first 250 m. From 500 to 1000 the models are biased high (50 to 100%) in the north-eastern and south-western directions. For the Dallas airport, the east-west positive bias (~20%) detected for all of the models in the first 250 m turns clockwise at 500 m, directed in the north-west direction. GEM and WRF-CAMx models also acquire a south-western bias component (about 70%) at 1000 m. The bias progressively decreases from 2 km up. At Frankfurt airport, the models share similar bias patterns: at the ground the tendency is to underestimate the occurrences of northerly winds (all models) and to overestimate the westerly components (with different magnitude by all models).

Finally we note that for the NA airports, the two instances of WRF do not always provide the same counts at all heights and at all locations. These two fields were derived from the same underlying WRF simulation. Therefore, the differences seen in this analysis were introduced when the two modelling groups independently interpolated these fields to the common horizontal and vertical analysis grid defined for the MOZAIC analysis under AQMEII and transferred these processed fields to ENSEMBLE. Thus, these differences highlight the difficulties in attributing differences in model performance to differences in model options, in particular for quantities with significant horizontal and vertical gradients such as wind direction.

4.2.3 Relative Humidity

In contrast to WS, modelled values of RH exhibit a smaller increase in variability with height and vary more by site than WS (Figure 4). The variability is underestimated by all models, as shown by the normalised standard deviation of Figure 4, most predominantly below unity at all airports, with the exception of Portland where the variability in the first 1000 m is close to the observed variability. The best model performance for variability occurs between 500 and 1000 m and deteriorates with height. As already mentioned, this could be due to the water vapour mixing ratio being very small aloft, making RH computation less reliable at higher altitudes. The analysis of the CoV reveals that there is a tendency to under-predict the observed variability in the free troposphere, especially for $z > 6$ km. Model performance is (as in the case of the WS) in general grouped by height, although with a few exceptions (such as the WRF/Chem at Frankfurt, Figure 4e). The minimum model errors and maximum PCC occur for altitudes in the range 1 to 3 km, although also with some exceptions (most notably Atlanta) and not consistently for all models. For example, the Taylor diagram for Frankfurt (Figure 4e) reveals a large scatter of data independent of height and model, with the same model performing well in some instances (LOTOS-EUROS at 3 km) but very poorly in others (the same model is off-scale at 0 m). Further investigation is needed to diagnose whether the modelled variation of RH is not ill-treated, or in other words if the modelling systems are getting the “correct answer for the right reason”, which is one of the main objective of the diagnostic model evaluation component defined in Dennis et al. (2010).

4.2.4 CO

Profiles of modelled CO show PCC values typically below 0.6 at all heights and airports, with a limited number of exceptions (e.g WRF-CMAQ at Frankfurt whose PCC above 3 km exceeds 0.7) (Figure 5a). All of the models show difficulty reproducing the temporal variability of CO concentrations, possibly due to the influence of local sources close to the airport whose temporal modulation is not captured by the models due to insufficiently fine grid spacing. Analysis of the CoV demonstrates that the variability is largely overestimated in the PBL at all NA airports (up to a factor of two at Dallas, Atlanta, and Philadelphia). CoV estimate improves slightly with height above the PBL, with the best agreement in the range of 2 to 4 km. This may be due to a stronger dependence on the large-scale transport from the BCs combined with the nudging of winds at these altitudes, while in the in the lower troposphere CO concentrations are the result of a more complex mix between transport and emission.

The analysis for CO was not separated by season but as there are more measurements available in summer than in winter, a bias to summer months is expected in the Taylor diagrams of Figure 5a. CO concentrations are typically lower in the spring and summer than in winter at all altitudes with a minimum in July and maximum in February to April (Gilge et al., 2010; Elguindi et al., 2010). As a result the annual mean deviation of the modelled to the observed profiles in Figure 2 and the error in Figure 5a are mostly associated with lower CO concentrations. Because model performance for CO is similar across all models, this may point to problems with the inputs that were largely shared among the models. In particular, the fact that at the ground the majority of models overestimate observed concentrations may indicate that emission from certain source categories such as mobile sources or biomass burning are overestimated. Another reason could be the emission profiles used: if CO is primarily emitted in the lowest layer, concentration at surface might result overestimated. This possibility could be checked by comparing the vertical profiles of other more long-lived substances, like aerosols. However, it is beyond the scope of this study to conclusively determine the reasons for the poor model performance near the surface.

Furthermore, one needs to consider that biased meteorological drivers might have a bigger impact on long lived species such as CO. The error in the input wind field (speed and direction) accumulates over time, possibly exacerbating errors introduced by imperfect emission inventories. To test this hypothesis for CO, we calculated the correlation between the error of the modelled CO concentration and the error of the WS at each given altitude and airport. Let $corr(f_{z,s1};g_{z,s2})$ be the operator returning the PCC of any two fields f and g at height z for the species s_1 and s_2, then $corr(e_{z,WS};e_{z,CO})$ is the PCC between the error of the WS at height z and the error of CO at the same height, whose profiles are reported in Figure 5b. From the graph it can be seen that there are instances for the NA airports where the two fields are largely positively correlated (up to values of ~0.3). Specifically, CAMx, AURAMS, and DEHM models for the Philadelphia airport for z = 500m and the WRF-CMAQ model at z = 3 km; the CCLM-CMAQ model for the Dallas airport for height up to 4km and all models for the Dallas airport for z between 3 and 4km. For these cases the errors of the two fields have the same trend. While a general trend is difficult to identify, there does appear to be a correlation between the fields for isolated model/airport/height combinations. Nonetheless, this analysis demonstrates that an association exists certain cases which deserve further investigations We also note that instances of anti-correlation (negative PCC) are also numerous, in these cases, a decreasing

error in WS corresponds an increasing error in CO and vice versa, but it is difficult to determine whether they are associated with vertical intrusion or should just be treated as uncorrelation. Finally, WS and CO errors at Frankfurt do not show any association and can be considered independent.

4.2.5 Ozone

Due to its adverse effects on human health, climate, and ecosystems, surface ozone is among the most extensively studied atmospheric trace gases. Solazzo et al. (2012a) have shown that overall the AQ modelling systems participating to AQMEII perform satisfactorily in reproducing ozone mixing ratios at ground level (showing better skill in NA than in EU). For most models and airports, the yearly averaged ozone scores of Figure 6 indicate better performance near the ground ($z \leq 1000$m) than aloft. At Portland the scores under and above the PBL are overall comparable and at Frankfurt several models have scores higher for altitude between 500 and 1000m (PCC in excess of 0.7) than for $z <$ 500m. The 1000 m height tends to mark a transition from the PBL regime, characterised by well-mixed dynamics and active photochemistry, to a tropospheric regime characterised by a more marked model-to-model variability. Similar conclusions were drawn by Chevalier et al. (2007).

No clear factor emerges for grouping the ozone skill scores in Figure 6. The two instances of CMAQ over NA (driven by WRF and CCLM), do not produce similar scores at any of the airports, although they share BCs and emissions. By contrast, CMAQ and CAMx, the two AQ models driven by WRF, share rather similar results, indicating that the meteorological driver may have a substantial weight in determining the skill for ozone (in particular PBL dynamics). However, this latter hypothesis is not confirmed by the Taylor plots for Frankfurt (WRF/Chem and CMAQ are both driven by WRF) though, as the scores are primarily grouped by AQ modelling system, with the two simulations of CMAQ producing similar scores.

The standard deviation and the CoV are generally overestimated within the PBL and underestimated aloft, although with several exceptions depending on the site, height, and model used, especially at the Atlanta, Dallas, and Frankfurt airports where the variability score at high altitudes is comparable to that in the PBL. WRF/Chem at Frankfurt shows the lowest variability at all heights, and close to zero for $z \geq 3$km, possibly because at these heights the simulated values are already influenced to some extent by the WRF/Chem BCs (constant values), which are too low particularly in the spring and summer at this range of height and also above (see Figure 2). The DEHM model underestimates the CoV at all NA airports, possibly due to the use of RCP emissions and different set of BCs (see Table 2).

The variability and errors above 3km and up to 8.5km reveals some model deficiencies. The mean seasonal profiles in Figure 2 indicated that the models tend to underestimate ozone between 3 and 6 km, but they overestimate ozone concentrations above that height (see Frankfurt for example), though not systematically for all locations and all seasons. This could be due to an under estimation of the exchange between the upper troposphere and the lower stratosphere and/or diffusive model errors related to coarse vertical gridding. By contrast, for the case of global scale chemistry models, Brunner et al. (2003), reported a tendency of models to overestimate ozone mixing ratios in the NA continental-scale domain between 5.5-8 km throughout the year (based on the period 1995-1998). However, while those results were averaged over the entire NA continent, here we are comparing

regional scale models at considerably smaller scales, and the different behaviour could simple be attributed to the different grid sizing as well as the different time period.

5. Altitudinal correlations

In this section we investigate the degree of association between the error at the ground (z = 0) with the error aloft (0 < z ≤ 8.5 km), measured by the PCC for each of the variables. With the terminology introduced in section 4.2.4, the association is expressed as $corr(e_{0,s}, e_{z,s})$, where s = (ozone, CO, WS, RH) and z's range is defined above. The intent of this analysis is to investigate whether errors in each field stem from sources and processes common to the surface and upper air. If errors at the ground and aloft are caused by independent processes, then we would expect the respective time series of errors to be uncorrelated. For example, if errors near the surface are primarily due to the treatment of PBL processes (photochemistry, deposition, emissions, turbulent mixing) these errors should not be correlated with errors further aloft. Conversely, in the case errors are due to the large scale circulation we would expect that under- or over-estimation is observed simultaneously at different altitudes, and therefore correlated.

Figure 8 reports how the fractional difference (FD) at the ground is correlated with the FD aloft for all investigated airports. FD is defined as:

$$FD = \frac{Mod - Obs}{0.5(Mod + Obs)} \quad (1)$$

where *Mod* and *Obs* are *N*-length vectors denoting the modelled and the observed field value, respectively. Here *N* is the number of hourly flights available for the period being analysed (reported in Table 1.). The correlations are calculated between the *N*-length FD vector at the ground with the *N*-length FD vector at other levels.

The profiles of FD correlations in
Figure 8 demonstrate that for the investigated fields (with some exceptions for CO as discussed below) positive correlations are limited to the PBL and that biases within the PBL are overall poorly correlated with those of the free troposphere, at all airports. The gradient of the correlation profiles drops sharply with height for both WS and RH. For these latter fields in particular we observe the strongest vertical gradient as well as the most homogeneous behaviour among the different models, suggesting that the proper simulation of WS and RH in the PBL is principally determined by near-surface processes (the only exception is WRF/WRF-Chem at Frankfurt).

Correlation of FD profiles for CO exhibits a less homogeneous behaviour. PCC varies aloft between 0.1-0.2 and 0.4-0.6, this latter value generally produced by MM5-DEHM for which the hypothesis of large scale error might explain the correlation between bias at the ground and aloft (note that DEHM results reflect the strong vertical mixing shown by the mean vertical profiles of Figure 2). Correlation of FD profiles for ozone is more homogeneous than CO among the different models, supporting the proposition that the vertical ozone profile is the result of an interplay between an ozone reservoir in the upper troposphere and ground level concentrations (Zhang and Rao, 1999; Godowitch et al.,

2011. Overall errors produced in the PBL for ozone remain contained within the PBL (all models show similar patterns) and are weakly connected with those above, although for Frankfurt this pattern is less pronounced. Above the PBL height, and especially for the two CMAQ simulations at Portland and WRF/Chem at Frankfurt, the FD correlation profiles are more varied, typically low for CAMx (goes very close to zero between 3 and 4km at all airports) and scattered between PCC values of 0 to 0.3 for the other models.

Although the altitudinal correlation analysis is very informative about how far the errors at the ground propagate in the vertical, it cannot be considered exhaustive as it does not provide detailed insight into the modelling systems' ability to represent specific processes. Instead, it reveals the need for a more quantitative evaluation of vertical mixing which could be accomplished, in first instance, by comparing the modelled PBL height with measurements, which were not collected within AQMEII.

6. Altitudinal error: the case of ozone

6.1 Aggregate seasonal error

The seasonal error associated with the model's capability in predicting ozone mixing ratios in the vertical is investigated for all airports and models. The error is expressed as fractional absolute difference (FAD):

$$FAD = \frac{|Mod - Obs|}{0.5(Mod + Obs)} \quad (2)$$

(the elements in Eq. 2 have been defined in Eq. 1). Results are presented for the winter months of December, January, and February (DJF, Figure 9) and for the summer months of June, July, and August (JJA, Figure 10) in terms of cumulative FAD. The bars in Figures 9 and 10 represent the sum of the errors produced by each model for that height. Since there are about twice the number of models for EU than for NA (9 vs. 5), one would expect the cumulative FAD of EU to be about twice that of NA. However this is not the case for the winter at Frankfurt where errors at the ground are more than double compared to the NA airports. Almost all of the models have large FAD at ground, pointing to some common problem (possibly biased emissions). With height the errors of CAMx and LOTOS-EUROS drop, while SILAM's remains high (Frankfurt, winter). By contrast, in the summer, cumulative FAD at Frankfurt is about twice that of Philadelphia and Dallas but approximately the same as Portland and Atlanta, where all of the models exhibit higher errors than at Philadelphia and Dallas (the AURAMS model has the highest FAD). The marked decreasing of FAD with height for summer (Figure 10) indicates that model discrepancies are mainly related to surface processes. Particularly, errors could stem from an overestimation of emissions in the surrounding area giving rise to an excess of ozone production by primary precursors. As for ozone, the underestimation of deposition processes could also be a source of error. Horizontal advection and photochemistry schemes are also possible causes of model-to-model discrepancies (Zyryanov et al., 2012). Furthermore, the error of the WRF-CMAQ model at the ground at Philadelphia in winter is larger than the other instance of CMAQ driven by CCLM, likely due to a higher titration effect. Figure 2 also shows that WRF-CMAQ exhibits the highest CO concentration, suggesting that differences between the two CMAQ simulations may be due to the difference in the vertical diffusion scheme used. Moreover, the

distribution of FAD of the CCLM-CMAQ model (negligible at ground and larger above 500 m) at Portland in winter and at Philadelphia and Dallas in summer, suggests that CCLM-CMAQ is able to capture the surface layer equilibrium between NOx and ozone, driven by titration, better than the other models. It is also worth noting that the performance of CCLM-CMAQ aloft is comparable with those of the other models, indicating that surface level processes are not strongly influenced by ozone aloft. Finally, the large error at 8.5 km at Frankfurt is due to model top boundary being close to that height, as for example the SILAM model.

Overall the diversity of modelling errors both in the PBL (particularly in summer) and in the free troposphere (particularly in winter) indicates a large range of differences in the AQ models, particularly at Frankfurt in both seasons. These differences relate to turbulence, transport, and photochemistry in the PBL (the emissions are largely shared), and to grid spacing, top and lateral boundary, and advection schemes in the free troposphere.

6.2 Bias due to Boundary Conditions

In this section we expand the model evaluation by providing comparison between the lateral BCs for ozone and the vertical profiles of ozone measured onboard MOZAIC aircraft. We show the analysis for NA only, as the proximity of the airports to the edges of the modelled domain allows testing the influence of the BCs more effectively. Details about the preparation of the standard BCs for AQMEII are given in Schere et al. (2012).

For the airports of Vancouver and Portland (west coast) and Philadelphia (east coast) we analyse the following hourly vertical profiles averaged over the months of January and August:

- monthly ozone BCs adopted by the AQ models;
- monthly profiles of modelled ozone concentration over the selected airports;
- monthly MOZAIC measurements of ozone at the selected airports and the observed standard deviation;
- ozonesonde data collected at rural locations falling within the MOZAIC domain for Philadelphia for the month of August 2006.

Results of the comparison are shown in Figure 12 to Figure 16. The GEMS BCs were adopted by the WRF-CMAQ, CCLM-CMAQ, and CAMx models (Table 2); the AURAMS group used its own BCs, while ozone BCs for DEHM were extracted from climatology and satellite measurements and applied to the model's outer domain which encompasses the entire northern hemisphere. The concentration profiles at the DEHM's inner domains (one centred in NA and one in EU), which reflect the dynamics of the hemispheric domain, are taken here for comparison (the cells where the profiles were extracted is shown in Figure 11).

During wintertime, the absence of strong photochemical activity amplifies the influence of BCs. For z > 2km the ozone monthly profiles on both the US coasts overlap to a large extent the corresponding boundary profiles (Figures 13-15). The only exception is for DEHM which shows a significant departure with altitude from the boundary profile and, consequently, also the bias with respect to the observed MOZAIC profiles reflects the error of the BCs for this model. For January at Vancouver and

Philadelphia, the modelled profiles have sharper gradients within the PBL than aloft due to the titration effect, but the ozone modelled concentrations clearly reflect the influence of BCs acting as an offset to surface concentrations, confirming that during wintertime the mean bias in ground level concentrations is mostly driven by the large scale background concentrations. This is further demonstrated by the correlation analysis in Figure 13, where we show the normalised bias of the BCs with respect to the MOZAIC versus the modelled ozone concentration with respect to MOZAIC. The regression analysis demonstrates the large degree of association between the bias of two fields (especially for AURAMS and WRF-CMAQ, with PCC of 0.86 and 0.75 respectively). When including only the bias of the levels from above 500m in the analysis, the PCC values are even larger for all models except AURAMS for which fewer data are available as the top of the model domain extends to only 5km. This confirms the findings of Schere et al. (2012) regarding the penetration of the bias induced by the BCs for ozone far into the interior of the model simulation domain. This was found to be especially true for the winter months and for rural areas away from major emission sources. Systematic underestimation of tropospheric ozone by the global modelling systems that was used to derive the boundary concentrations for the AQMEII modelling caused the regional-scale models to often underestimate near surface ozone concentrations in NA.

Different behaviour is observed in summer. At Portland (Figure 14) all models underestimate the observed concentration above 2 km, with the GEMS BCs also underestimating the MOZAIC measurements. Below 1000 m, all models overestimate the observed concentrations of ~20-25 ppb, possibly because of the overestimation of vertical mixing in the PBL. It should be further noted that the distance between Portland and the coast is of ~100km, and therefore the grid cell over the airport should not include any ocean area (model grid spacings are well below 100 km) and thus there should not be any gradient between deposition over ocean and over land, leading to overestimation of modelled ozone. At 1000 m height the bias between models and MOZAIC is at smallest before turning to positive at 2km, with the modelled profiles unable to replicate the sharp gradient in the MOZAIC data. Such a gradient is possibly due to the titration effect of NO_X surface emissions together with surface deposition. Although the aircrafts fly rapidly away from/to the airport the urban influences of the large urban area around the airport is expected to increase the ozone gradient in the lowest levels due to fast titration by NO. This effect is expected to vanish aloft (Chevalier et al., 2007). Differences in the aloft boundary concentrations profiles are also seen in the aloft modelled values and in turn in the ground level concentrations. This is not the case for DEHM, where, once again, the vertical mixing appears to play the dominant role. Overall, the BCs do not appear to be the primary driver for the bias on the west NA coast during summer.

At the Philadelphia airport, the models tend to slightly underestimate (5 to 10 ppb) ozone concentrations for the month in August 2006 (Figure 16) above 4 km, while there is an overestimation below 1000m by 6 to 20 ppb. The models driven by the BCs provided by GEMS and, to a lesser extent, AURAMS replicate very well the observed profile between 1.5 and 3 km, while DEHM is biased high. GEMS profiles are biased low above 4000m and in agreement with MOZAIC at ground up to 1.5km. The models driven by the GEMS BCs (the two instances of CMAQ and CAMx) show some differences within the first 3 km, though they cluster around the corresponding boundary value in the upper levels. The bias at these altitudes is possibly influenced by the GEMS BCs. The spread among the models is likely driven by photochemistry, the effect of which is stronger in Philadelphia than

Portland, being the east coast subject to higher NOx emission loads than the western areas (see e.g., Appel et al., 2012). Ground level ozone concentrations simulated from models driven by GEMS range between 45 and 65 ppb, consistent with the notion that local production enhances summer ozone concentrations in polluted areas over more than large scale background concentrations. This result is also shared by DEHM which exhibits the highest surface concentrations, although it was fed by the lowest boundary concentration values. Profiles of ozone concentration measured by ozonesondes for the month of August were available from two rural sites (Figure 11) within the Philadelphia domain, and are reported in Figure 16. Measurements at the site STN487 (~370km north-east of the airport, close to the coast) were collected daily for the month of August at 18 GMT, while there are 12 hourly measurements from the STN420 (~160km south-west of the airport), collected at different hour of the day, between 04 GMT and 20 GMT. Profiles of STN420 are similar to those of the MOZAIC in the first 1000m but diverge from the modelled concentration more than the MOZAIC above 1000m. The profiles from this rural ozonesonde station therefore suggest that the GEMS BCs may be biased low at this site (also found by Schere et al., 2012). Values of ozone concentration reported by the other station STN487 also support this inference as they are close to the MOZAIC values in the upper levels. Finally, ozonesonde profiles from both sites confirm that the modelled ozone concentrations are biased high in the first 1000m.

7. Summary and Conclusions

This study has been conducted in the framework of the AQMEII activity and presents an evaluation of regional scale AQ models in the troposphere supported by measurements gathered in the MOZAIC campaign. Fifteen regional scale modelling groups from EU and NA have produced three dimensional data of ozone, CO, WS, WD, RH and temperature with hourly resolution for the full year of 2006 at selected areas around major airports in EU and NA. These data have been paired with MOZAIC vertical profiles by the ENSEMBLE platform.

The scope of this study is the operational evaluation of the AQ modelling systems, i.e. the comparison of model results to observed data, supported by error metrics and variance statistics to gauge model performance in an overall sense. Results are thus based on the operational statistics obtained by comparing modelled against measured profiles. Several cases exhibiting significant differences between observations and model predictions have been identified as potential subjects of more in-depth diagnostic analysis to be undertaken in future.

From the study of the annual average mean vertical profiles of WS we conclude:

- Above the PBL, there is little model-to-model variability at all airports, with all models showing similar mean profiles, most likely because of the influence of nudging. MM5-DEHM is the only model showing a positive bias for WS which increases with altitude at all sites, likely due to the coarser grid spacing used
- For winds within the PBL (which are not nudged), all models (at all airports) show significant errors (predominantly as a positive bias) and poor correlation with the observed WS values in the first 100 m, and generally up to 500 m, with smaller errors between 500 and 1000 m. In addition, most models underestimated the variability within the first 100 m at all airports, indicating that the meteorological models are still weak in reproducing WS in the PBL. Factors that could contribute to

the poor performance include sensitivity of the near-surface winds to influences other than the synoptic circulation (e.g. land cover), and processes driving the exchange of energy at surface for which global and regional models are known to largely differ from one another. For all models and at all airports, PCC, error and variability improve consistently with altitude. In general, the best performance by all models are observed for $z \geq 3$ km with a PCC > 0.8 at all NA airports and, with the exception of the WRF/Chem model (PCC~0.65 at z=3 km), at Frankfurt as well.

We also investigated the model-to-model bias in predicting the frequency of WD counts when the whole wind rose is binned into 20° intervals, at all heights. We find that:

- The bias in the PBL at Frankfurt is smaller and decreases faster with height with respect to the other NA airports, for which larger biases are found, most pronounced at Portland (west NA coast), where positive bias of 80% (south-east sectors) is found for $0 \leq z \leq 500$ m for GEM and WRF/Chem;
- Overall, the bias at NA airports tends to decrease above 3 km, while it is significant in the first 250 to 500m (depending on the airport), and is predominantly associated to over-prediction of westerly winds.

A further meteorological variable evaluated in this study is RH for which we find:

- RH profiles are layered with height and agree satisfactorily with the observations within the first ~2 km, but significantly diverge above that height at all sites. We attribute such discrepancy to the low values of water vapour mixing ratio at those heights for which small differences in temperature can give rise to significant differences in RH. The RH peaks at 1000 m at all airports, although with different magnitudes. The peak is generally well captured by the models at all airports, with the exception of Dallas where the models bias at 1000m ranges between 7 to 15%.
- Model performance for RH is found to be site-dependant and a general trend could not be identified, although PCC values are above 0.5 at all NA sites and, with the exception of WRF/Chem, also at Frankfurt.
- Variability tends to be underestimated by all models (especially for z > 6km) with the exception of Portland where the variability in the first 1000m is close to the observed variability.

Model performance for temperature is satisfactory for all models and airports for, the first 5km (PCC in excess of 0.90 and fractional bias ≤ 1%).

The chemical species investigated in this study are CO and ozone. We find modelled CO to show the largest range of modelled-to-observed standard deviations detected in this study, at all heights, for all airports. Correlation for CO is typically below 0.6 at all airports and all heights, with very few exceptions. Errors are also large at all altitudes and mainly in the first 250 m. Because the errors are common to all models, it is possible that one or more of the inputs shared by the models is biased, most likely the emissions. Performance improves slightly with height, giving the best scores in the range of altitudes between 2 and 4 km. With respect to the impact of WS errors on CO errors, there are instances for the NA airports where the WS and CO errors are correlated, with the same general trend. However, the correlations only exist for at certain models at particular airports and heights.

Ozone concentration profiles are strongly dependent on surface processes, as revealed by the strong gradient in the first 2 km of the troposphere, ranging on average between 10 to 20 ppb/km at all sites. Modelled ozone in winter is typically biased low at all locations, with the exception of DEHM for both NA and EU. Ozone within the PBL is generally overestimated in summer (NA only), whit better performance in fall, especially for Frankfurt. Layered ozone profiles are most notable in the summer months close to the surface, likely as result of the photochemistry and thermal mixing. Overall model performance for ozone in the PBL can be considered satisfactory (with bias and error within 20%).

The impact of BCs on the ozone is examined by comparing observed ozone profiles to model profiles at NA airports close to the model boundary, where the effect from the boundary would be the largest. While the BCs determine the bias of the modelled profiles for winter on both coasts, for summer the near-surface effects (e.g. photochemistry, transport, emissions, and deposition) dominate the ozone mixing ratios, lessing the impact from the BCs. However, on the east coast for the summer, a non-negligible influence from the BCs on the free-tropospheric ozone cannot be excluded. Finally, an analysis of the correlation between the bias at the ground with that aloft conducted for all variables demonstrates that, with the possible exception of CO, the errors produced in the PBL are weakly associated with those above, indicating that errors near the surface are primarily due to the treatment of PBL processes.

Suggestions for future work include interpretation of the model-to-model variability and common sources of model bias, and linking CO and ozone bias to the bias in the meteorological fields.

Acknowledgements and disclaimer
The MOZAIC Data Centre and its contributing airlines provided North American and European aircraft takeoff and landing vertical profiles are kindly acknowledged. The WMO World Ozone and Ultraviolet Data Centre (WOUDC) and its data contributing agencies provided North American and European ozonesonde profiles. GY and UN acknowledge financial support from the Coordinating Research Council Atmospheric Impacts Committee (Project A-75) and the Electric Power Research Institute. The contribution of RSE SpA to this work has been partially financed by the Research Fund for the Italian Electrical System under the Contract Agreement between RSE SpA and the Italian Ministry of Economic Development (Decree of March 19th, 2009).

Although this work has been reviewed and approved for publication by the U.S. Environmental Protection Agency, it does not reflect the views and policies of the agency.

References

Appel, K.W., Bhave, P.V., Gilliland, A.B., Sarwar, G., Roselle, S.J., 2008. Evaluation of the Community Multiscale Air Quality (CMAQ) model version 4.5: Sensitivities impacting model performance; Part II - particulate matter, Atmospheric Environment (2008).

Appel, K.W., Gilliand, A.B., Sarwar, G., Gilliam, R.C., 2007. Evaluation of the Community Multiscale Air Quality (CMAQ) model version 4.5: Sensitivities impacting model performance; Part I - ozone, Atmospheric Environment.

Appel, W., Chemel, C., and et al. 2012. Examination of the Community Multiscale Air Quality (CMAQ) model performance for North America and Europe for the AQMEII project. Atmospheric Environment 53, 142-155.

Aulinger, A., Matthias, V., Quante, M. (2011). An approach to temporally disaggregate Benzo (a) pyrene emissions and their application to a 3D Eulerian atmospheric chemistry transport model, Water Air and Soil Pollution, 216, 643-655

Bélair, S., Mailhot, J., Strapp, J.W., MacPherson, J.I. (1999). An examination of local versus nonlocal aspects of a TKE-based boundary-layer scheme in clear convective conditions. J. Appl. Meteor., 38, 1499-1518.

Benoit, R., Côté, J., Mailhot, J. (1989). Inclusion of TKE boundary-layer parameterization in the Canadian regional finite-element model. Mon. Wea. Rev. 117, 1726-1750.

Bessagnet, B., Hodzic, A., Vautard, R., Beekmann, M., Cheinet, S., Honoré, C., Liousse, C., Rouil, L., 2004. Aerosol modeling with CHIMERE: preliminary evaluation at the continental scale. Atmospheric Environment 38, 2803-2817.

Bessagnet, B., Seigneur, C., Menut, L., 2010. Impact of dry deposition of semi-volatile organic compounds on secondary organic aerosols. Atmospheric Environment 44 1781-1787, ISSN 1352-2310, 10.1016/j.atmosenv.2010.01.027.

Blond, N., and R. Vautard, 2004: Three-dimensional ozone analyses and their use for short-term ozone forecasts, J. Geophys. Res., doi:10.1029/2004JD004515.

Bond, T.C., E. Bhardwaj, R. Dong, R. Jogani, S. Jung, C. Roden, D.G. Streets, S. Fernandes, and N. Trautmann (2007), Historical emissions of black and organic carbon aerosol from energy-related combustion, 1850-2000, Glob. Biogeochem. Cyc., 21, GB2018

Boynard, A., Beekmann, M., Foret, G., Ung, A., Szopa, S., et al., 2011. An ensemble assessment of regional ozone model uncertainty with an explicit error representation. Atmospheric Environment 45, 784-793.

Brandt, J., J. D. Silver, L. M. Frohn, C. Geels, A. Gross, A. B. Hansen, K. M. Hansen, G. B. Hedegaard, C. A. Skjøth, H. Villadsen, A. Zare, and J. H. Christensen, 2012: An integrated model study for Europe and North America using the Danish Eulerian Hemispheric Model with focus on intercontinental transport. Atmospheric Environment 53, 156-176

Brunner, D., Staehelin, J., Rogers, H.L., et al., 2003. An evaluation of the performance of chemistry transport models by comparison with research aircraft observations. Part 1: Concepts and overall model performance. Atmos Chem. Phys. 3, 1609-1631

Brunner, D., Staehelin, J., Rogers, H.L., et al., 2005. An evaluation of the performance of chemistry transport models – Part 2: Detailed comparison with two selected campaigns. Atmos Chem. Phys. 5, 107-129

Byun, D., Schere, K.L., 2006. Review of the Governing Equations, Computational algorithms, and other components of the Models-3 community Multiscale air quality (CMAQ) modeling system. Applied Mechanics Reviews 59, 51-77.

Carlton, A.G., Bhave, P.V., Napelenok, S.L., Edney, E.O., Sarwar, G., Pinder, R.W., Pouliot, G.A., Houyoux, M., 2010. Model representation of secondary organic aerosol in CMAQv4.7. Environmental Science and Technology 44, 8553-8560

Chevalier, A., Gheusi, F., Delmas, R., and et al. 2007. Influence of altitude on ozone levels and variability in the lower troposphere : a ground based study for western Europe over the period 201-2004. Atmos Chem. Phys. 7, 4311-4326

Christensen, J. H., 1997. The Danish Eulerian Hemispheric Model – a three-dimensional air pollution model used for the Arctic, Atm. Env., 31, 4169–4191.

Colella, P., Woodward, P. R. (1984). The Piecewise Parabolic Method (ppm) For Gas-dynamical Simulations, Journal of Computational Physics **54**(1), 174--201.

Corbett, J. J. and P. S. Fischbeck, 1997: Emissions from ships. Science, 278:823–824

Côté, J., Desmarais, J.-G., Gravel, S., Méthot, A., Patoine, A., Roch, M., Staniforth, A., 1998a. The operational CMC/MRB Global Environmental Multiscale (GEM) model. Part I: Design considerations and formulation. Monthly Weather Review 126, 1373-1395.

Côté, J., Desmarais, J.-G., Gravel, S., Méthot, A., Patoine, A., Roch, M., Staniforth, A., 1998b. The operational CMC/MRB Global Environmental Multiscale (GEM) model. Part II: Results. Monthly Weather Review 126, 1397-1418.

Cros, B., Durand, P., Frejafon, E., Kottmeier, C., Perros, P., Peuch, V-H., Ponche, J-L., Robin, D., Said, F., Toupance, G., Wotham,H., 2004. The ESCOMPTE program: an overview, Atmos. Res. 69, 241–279

De Noblet-Ducoudré, N., J.-P. Boissier, A. Pitman, G. B. Bonan, V. Brovkin, F. Cruz, C. Delire, V. Gayler, B. van den Hurk, P. J. Lawrence, M. K. van der Mollen, C. Müller, C. H. Reick, B. J. Strengers & A. Voldoire, 2012. Determining Robust Impacts of Land-Use-Induced Land Cover Changes on Surface Climate over North America and Eurasia: Results from the First Set of LUCID Experiments. J. Climate, 25, 3261-3281.

Dennis, et al., 2010. A framework for evaluating regional-scale numerical photochemical modelling systems. Environmental Fluid Mechanics. doi:10.1007/s10652-009-9163-2.

Drobinski, P., F. Saïd, G. Ancellet, J. Arteta, P. Augustin, S. Bastin, A. Brut, J.L. Caccia, B. Campistron, S. Cautenet, A. Colette, B. Cros, U. Corsmeier, I. Coll, A. Dabas, H. Delbarre, A. Dufour, P. Durand, V. Guénard, M. Hasel, N. Kalthoff, C. Kottmeier, A. Lemonsu, F. Lohou, V. Masson, L. Menut, C. Moppert, V.H. Peuch, V. Puygrenier, O. Reitebuch, R. Vautard, 2007: Regional transport and dilution during high pollution episodes in southeastern France: summary of findings from the ESCOMPTE experiment. J. Geophys. Res., 112, D13105, doi:10.1029/2006JD007494.

Elguindi, N., C. Ordonez, V. Thouret, J. Flemming, O. Stein, V. Huijnen, P. Moinat, A. Inness, V.-H. Peuch, A. Stohl, S. Turquety, J.-P. Cammas, M. Schultz, 2010. Current status of the ability of the GEMS/MACC models to reproduce the tropospheric CO vertical distribution as measured by MOZAIC, *Geoscientific Model Development 3, 501–518*.

Emeis, S., Forkel, R., Junkermann, W., Schafer, K., Flentje, H., Gilge, S., Fricke, W.,Wiegner, M., Freudenthaler, V., Gross, S., Ries, L., Meinhardt, F., Birmili, W., Münkel, C., Obleitner, F., Suppan, P., 2011. Measurement and simulation of the 16/17 April 2010 Eyjafjallajökull volcanic ash layer dispersion in the northern Alpine region. Atmospheric Chemistry and Physics 11 (6), 2689-2701 (doi:10.5194/acp-11-2689-2011)

Emery C.A., E. Tai, G. Yarwood, R. Morris. 2011. Investigation into approaches to reduce excessive vertical transport over complex terrain in a regional photochemical grid model. Atmospheric Environment, 45, 7341-7351. DOI: 10.1016/j.atmosenv.2011.07.052

ENVIRON, 2010. User's Guide to the Comprehensive Air Quality Model with Extensions (CAMx) version 5.20. Available at http://www.camx.com.

Fisher, H., Lawrence, M., Gurk, Ch., Hoor,P., and et al 2006.model simulations and aircraft measurements of vertical, seasonal and latitudinal O3 and CO distribution over Europe. Atmos Chem. Phys. 6, 339-348

Foley, K.M., Roselle, S.J., Appel, K.W., Bhave, P.V., Pleim, J.E., Otte, T.L., Mathur, R., Sarwar, G., Young, J.O., Gilliam, R.C., Nolte, C.G., Kelly, J.T., Gilliland, A.B., Bash, J.O., 2010. Incremental testing of the Community Multiscale Air Quality (CMAQ) modeling system version 4.7. Geoscientific Model Development 3, 205-226.

Forester, C.K. (1977). Higher order monotonic convective difference schemes. Journal of Computional Physics, 23, 1-22

Forester, C.K., 1977. Higher order monotonic convective difference schemes. J. Comput. Phys. 23, 1-22.

Forkel, R.,Werham, J., Hansen, A.B., McKeen, S., Peckam, S., Grell, G., Suppan, P., 2012. Effect of aerosol-radiation feedback on regional air quality - A case study with WRF/Chem. Atmospheric Environment 53, 202-211.

Frohn, L. M., J. H. Christensen and J. Brandt, 2002. Development of a high resolution nested air pollution model – the numerical approach. Journal of Computational Physics. Vol. 179, 68-94.

Galmarini, S., Bianconi, R., Addis, R., Andronopoulos, S., Astrup, P., Bartzis, J.C., Bellasio, R., Buckley, R., Champion, H., Chino, M., D'Amours, R., Davakis, E., Eleveld, H., Glaab, H., Manning, A., Mikkelsen, T., Pechinger, U., Polreich, E., Prodanova, M., Slaper, H., Syrakov, D., Terada, H., Van der Auwera, L., 2004. Ensemble dispersion forecasting, Part II: application and evaluation. Atmos. Environ. 38 (28), 4619e4632.

Galmarini, S., R. Bianconi, W. Appel, E. Solazzo, S. Mosca, P. Grossi, M. Moran, K. Schere, and S.T. Rao, 2012. ENSEMBLE and AMET: Two systems and approaches to a harmonized, simplified and efficient facility for air quality models development and evaluation. Atmos. Environ. 53, 51-59.

Galperin, M. V. (1999), Approaches for improving the numerical solution of the advection equation, in Large-Scale Computations in Air Pollution Modelling, edited by Z. Zlatev et al., pp. 161–172, Kluwer Acad., Dordrecht, Netherlands.

Galperin, M. V. (2000), The approaches to correct computation of airborne pollution advection, in Problems of Ecological Monitoring and Ecosystem Modelling (in Russian), vol. XVII, pp. 54–68, Gidrometeoizdat, St. Petersburg, Russia.

Gazdag, J., Numerical convective schemes based on accurate computation of space derivatives. Journal of Computational Physics, 13 (1973), pp. 100-113

Gilge, S., Plass-Duelmer, C., Fricke, W., and et al., 2010. Ozone, carbon monoxide and nitrogen oxides time series at four alpine GAW mountain stations in central Europe. Atmos Chem. Phys. 10, 2295-12316

Godowitch, J.M., R C. Gilliam, and S. T. Rao, 2011, Diagnostic evaluation of ozone production and horizontal transport in a regional photochemical air quality modeling system, Atmospheric Environment, 45, 3977-3987

Gong, W., Dastoor, A.P., Bouchet, V.S., Gong, S., Makar, P.A., Moran, M.D., Pabla, B., Ménard, S., Crevier, L.-P., Cousineau, S., Venkatesh, S., 2006. Cloud processing of gases and aerosols in a regional air quality model (AURAMS). Atmospheric Research 82, 248-275

Graedel, T.E., T.S. Bates, A.F. Bouwman, D. Cunnold, J. Dignon, I. Fung, D.J. Jacob, B.K. Lamb, J. A. Logan, G. Marland, P. Middleton, J.M. Pacyna, M. Placet, and C. Veldt (1993): A Compilation of Inventories of Emissions to the Atmosphere. Global Biogeochemical Cycles. 7, 1-26.

Grell, G.A., Peckham, S.E., Schmitz, R., McKeen, S.A., Frost, G., Skamarock, W.C., Eder, B., 2005. Fully coupled online chemistry within the WRF model. Atmospheric Environment 39, 6957-6975.

Guenther, A., Karl, T., Harley, P.,Wiedinmyer, C., Palmer, Geron, C., 2006. Estimates of global terrestrial isoprene emissions using MEGAN (Model of Emissions of Gases and Aerosols from Nature), Atmos. Chem Phys., 6, 3181-3210.

Guenther, A., Zimmerman, P., Wildermuth, M., 1994. Natural volatile organic compound emission rate estimates for US woodland landscapes. Atmos. Environ., 28, 1197–1210.

Hong, S.Y., Noh, Y., Dudhia, J., 2006. A new vertical diffusion package with an explicit treatment of entrainment processes. *Monthly Weather Review*, 134, 2318-2341.

Jonson, J.E., Stohl, A., Fiore, A.M., and et al., 2010. A multi-model analysis of vertical ozone profiles. Atmospheric Chemistry and Physics 10, 5759-5783.

Lamarque, J.F., Bond, T.C., Eyring, V., Granier, C., Heil, A., Klimont, Z., Lee, D., Liousse, C., Mieville, A., Owen, B., Schultz, M.G., Shindell, D., Smith, S.J., Stehfest, E., Van Aardenne, J., Cooper, O.R., Kainuma, M.,

Mahowald, N., McConnell, J.R., Naik, V., Riahi, K., Van Vuuren, D.P., 2010. Historical (1850-2000) gridded anthropogenic and biomass burning emissions of reactive gases and aerosols: Methodology and application. Atmospheric Chemistry and Physics Discussions 10, 4963-5019.

Logan, J.A., 1999. An analysis of ozonesonde data for the troposphere: recommendations for testing 3-D models, and development of a gridded climatology for tropospheric ozone. Journal of Geophysical Research 104 (16), 115-116.

Louis, J., 1979. A parametric model of vertical eddy fluxes in the atmosphere. Boundary-Layer Meteorology, 17, 197-202.

Mailhot, J., Bélair, S., Lefaivre, L., Bilodeau, B., Desgagné, M., Girard, C., Glazer, A., Leduc, A.-M., Méthot, A., Patoine, A., Plante, A., Rahill, A., Robinson, T., Talbot, D., Tremblay, A., Vaillancourt, P., Zadra, A., Qaddouri, A. (2006). The 15-km version of the Canadian regional forecast system. Atmosphere - Ocean, 44, 133-149.

Marenco, A., and et al., 1998. Measurement of ozone and water vapor by Airbus in-service aircraft: the MOZAIC airborne program, an overview. Journal of Geophysical Research 103, 670-694.

Matthias, V., Aulinger, A., Bieser, J., Cuesta, J., Geyer, B., Langmann, B., Serikov, I., Mattis, I., Minikin, A., Mona, L., Quante, M., Schumann, U., Weinzierl, B. (2012): "The ash dispersion over Europe during the Eyjafjallajökull eruption – Comparison of CMAQ simulations to remote sensing and air-borne in-situ observations". Atmospheric Environment, 48, 184-194 (doi 10.1016/j.atmosenv.2011 06.077)

Matthias, V.; Bewersdorff, I.; Aulinger, A. & Quante, M. (2010). The contribution of ship emissions to air pollution in the North Sea regions, Environmental Pollution **158**(6), 2241-2250

Pepper, D.W., C.D. Kern and P.E. Long, Modeling the dispersion of atmospheric pollution using cubic splines and chapeau functions. Atmospheric Environment, 13 (1979), pp. 223-237

Pleim, J. E., Chang, J. S. (1992). A Nonlocal Closure-model For Vertical Mixing In the Convective Boundary-layer, Atmospheric Environment Part A-general Topics **26**(6), 965-981.

Pleim, J.E., 2007a. A combined local and nonlocal closure model for the atmospheric boundary layer. Part I: model description and testing. Journal of Applied Meteorology and Climate 46, 1383-1395.

Pleim, J.E., 2007b. A combined local and nonlocal closure model for the atmospheric boundary layer. Part II: application and evaluation in a mesoscale meteorological model. Journal of Applied Meteorology and Climate 46, 1396-1409.

Pouliot, G., T. Pierce, H. Denier van der Gon, M. Schaap, M. Moran, and U. Nopmongcol, 2012. Comparing emission inventories and model-ready emission datasets between Europe and North America for the AQMEII project. Atmos. Environ., 53, 4-14.

Pudykiewicz, J.A., Kallaur, A., Smolarkiewicz, P.K. (1997). Semi-Lagrangian modelling of tropospheric ozone, Tellus, 49B, 231-248.

Rao, S.T., Galmarini, S., Puckett, K., 2011. Air Quality Model Evaluation International Initiative (AQMEII). Bulletin of the American Meteorological Society 92, 23-30. DOI:10.1175/2010BAMS3069.1

Sartelet, K., Couvidat, F., Seigneur, C., Roustan, Y., 2012. Impact of biogenic emissions on air quality over Europe and North America. Atmospheric Environment 53, 131-141.

Schaap, M., F. Sauter, R.M.A. Timmermans, M. Roemer, G. Velders, J. Beck, P.J.H. Builtjes, 2008. The LOTOS-EUROS model: description, validation and latest developments, Int. J. Environment and Pollution, Vol. 32, No. 2, pp.270–290

Schere, K., Flemming, J., Vautard, R., Chemel, C., et al. Trace Gas/Aerosol concentrations and their impacts on continental-scale AQMEII modelling sub-regions. Atmospheric Environment 53, 38-50.

Simpson, D., A. Guenther, C. N. Hewitt, R. Steinbrecher, 1995. Biogenic emissions in Europe. 1. Estimates and uncertainties. J. Geophys. Res., 100D, 22875–22890.

Skamarock, W.C., Klemp, J.B., Dudhia, J., Gill, D.O., Barker, D.M., Duda, M.G., Huang, X.Y., Wang, W., Powers, J.G., 2008. A Description of the Advanced Research WRF Version 3. Technical Note NCAR/TN-475 þ STR.

Available from:. National Center for Atmospheric Research, Boulder, Colorado www.mmm.ucar.edu/wrf/users/docs/arw_v3.pdf, 113 pp.

Smith, S. J., Pitcher, H., and Wigley, T.M.L., 2001. Global and Regional Anthropogenic Sulfur Dioxide Emissions. Global and Planetary Change, 29, pp 99-119

Smith, S.J., Pitcher, H., Wigley, T.M.L., 2001. Global and regional anthropogenic Sulfur Dioxide emissions. Global and Planetary Change 29, 99-119

Smyth, S.C., Jiang, W., Roth, H., Moran, M.D., Makar, P.A., Yang, F., Bouchet, V.S., Landry, H., 2009. A comparative performance evaluation of the AURAMS and CMAQ air quality modelling systems. Atmospheric Environment 43, 1059-1070.

Sofiev, M. (2002), Extended resistance analogy for construction of the vertical diffusion scheme for dispersion models, J. Geophys. Res., 107(D12), 4159, doi:10.1029/2001JD001233.

Sofiev, M., E.Genikhovich, P.Keronen, and T.Vesala (2010), Diagnosing the surface layer parameters for dispersion models within the meteorological-to-dispersion modelling interface, J. Appl. Meteorol. Climatol., 49,221–233, doi:10.1175/2009JAMC2210.1.

Sofiev, M., M. Galperin, and E. Genikhovich (2008), Construction and evaluation of Eulerian dynamic core for the air quality and emergency modelling system SILAM, in Air Pollution Modelling and Its Application XIX, NATO Sci. Peace Security Ser. C: Environ. Security,editedby C. Borrego and A. I. Miranda, pp. 699–701, Springer, New York.

Solazzo, E., R. Bianconi, G. Pirovano, V. Matthias, R. Vautard, M.D. Moran, K.W. Appel, B. Bessagnet, J. Brandt, J.H. Christensen, C. Chemel, I. Coll, J. Ferreira, R. Forkel, X.V. Francis, G. Grell, P. Grossi, A.B. Hansen, C. Hogrefe, A.I. Miranda, U. Nopmongco, M. Prank, K.N. Sartelet, M. Schaap, J.D. Silver, R.S. Sokhi, J. Vira, J. Werhahn, R. Wolke, G. Yarwood, J. Zhang, S.T. Rao, and S. Galmarini, 2012b. Operational model evaluation for particulate matter in Europe and North America in the context of AQMEII. Atmos. Environ., 53, 75-92.

Solazzo, E., R. Bianconi, R. Vautard, K.W. Appel, M.D. Moran, C. Hogrefe, B. Bessagnet, J. Brandt, J.H. Christensen, C. Chemel, I. Coll, H. Denier van der Gon, J. Ferreira, R. Forkel, X.V. Francis, G. Grell, P. Grossi, A.B. Hansen, A. Jericevic, L. Kraljevic, A.I. Miranda, U. Nopmongcol, G. Pirovano, M. Prank, A. Riccio, K.N. Sartelet, M. Schaap, J.D. Silver, R.S. Sokhi, J. Vira, J. Werhahn, R. Wolke, G. Yarwood, J. Zhang, S.T. Rao, and S. Galmarini, 2012a. Model evaluation and ensemble modelling of surface-level ozone in Europe and North America in the context of AQMEII. Atmos. Environ., 53, 60-74.

Stegehuis, A., R. Vautard, P. Ciais, R. Teuling, M. Jung & P. Yiou (2012) Summer temperatures in Europe and land heat fluxes in observation-based data and regional climate model simulations. Climate Dynamics, submitted.

Stevenson, D.S., Dentener, F.J., Schultz, M.G., and et al., 2006. Multimodel ensemble simulations of present day and near future tropospheric ozone. Journal of Geophysical Research 111, D08301

Szykman, J., Solazzo, E., Cooper, O., Silverman, S., Trepte, C., Newchurch, M., Cammas, J.-P., Volz-Thomas, A., 2012. Profiles and remote sensing observation datasets for regional-scale model evaluation under the AQMEII North American and European perspectives. Environmental Manager, July 2012, 21-29

Taylor, K.E., 2001. Summarising multiple aspects of model performance in a single diagram. Journal of Geophysical Research 106, 7183e7192..

Thouret, V., Marenco, A., Logan, J.A., Nedelec, P., Grouhel, C., 1998. Comparison of ozone measurements from the MOZAIC airborne program and the ozone sounding network at eight locations. Journal of Geophysical Research 103, 695-720.

Troen, I. and Mahrt, L. (1986). A simple model of the atmospheric boundary layer: Sensitivity to surface evaporation. Bound.-Layer Meteorol., 37:129–148

Tulet, P., Suhre,K., Mari,C., Solomon,F., Rosset, R., 2002. Mixing of boundary layer upper tropospheric ozone during a deep convective event over Western Europe. Atmospheric Environment 36, 4491-4501.

Van Leer, B.: Towards the ultimate conservative difference scheme. A second order sequel to Godunov's method, J. Computational Phys., 32, 101–136, 1979

van Loon, M., Vautard, R., Schaap, M., Bergström, R., Bessagnet, B., Brandt, J., et al., 2007. Evaluation of long-term ozone simulations from seven regional air quality models and their ensemble average. Atmospheric Environment 41, 2083-2097.

Vautard, R., M.D. Moran, E. Solazzo, R.C. Gilliam, V. Matthias, R. Bianconi, C. Chemel, J. Ferreira, B. Geyer, A.B. Hansen, A. Jericevic, M. Prank, A. Segers, J.D. Silver, J. Werhahn, R. Wolke, S.T. Rao, and S. Galmarini, 2012. Evaluation of the meteorological forcing used for the Air Quality Model Evaluation International Initiative (AQMEII) air quality simulations. Atmos. Environ., 53, 15-37.

Vautard, R., Schaap, M., Bergström, R., Bessagnet, B., Brandt, J., Builtjes, P.J.H., Christensen, J.H., Cuvelier, C., Foltescu, V., Graf, A., Kerschbaumer, A., Krol, M., Roberts, P., Rouïl, L., Stern, R., Tarrason, L., Thunis, P., Vignati, E., Wind, P., 2009. Skill and uncertainty of a regional air quality model ensemble. Atmospheric Environment 43, 4822e4832.

Vestreng V, Støren E. Analysis of the UNECE/EMEP Emission Data. MSC-W Status Report 2000. Norwegian Meteorological Institute: Blindern, Oslo; 2000.

Walcek, C.J., 2000. Minor flux adjustment near mixing ratio extremes for simplified yet highly accurate monotonic calculation of tracer advection', J. Geophyical Res., Vol. 105, D7, pp.9335–9348.

Wei Tang, Daniel S. Cohan, Gary A. Morris, Daewon W. Byun, Winston T. Luke, Influence of vertical mixing uncertainties on ozone simulation in CMAQ, Atmospheric Environment, Volume 45, Issue 17, June 2011, Pages 2898-2909, ISSN 1352-2310, 10.1016/j.atmosenv.2011.01.057.

Yarwood, G., Rao, S., Yocke, M., Whitten, G., 2005. Updates to the Carbon Bond Chemical Mechanism: CB05. US EPA report RT-0400675. Available at http://www.camx.com.

Yu, S. C., Mathur, R., Kang, D., Schere, K., Pleim, J., and Otte, T. L.: A detailed evaluation of the Eta-CMAQ forecast model performance for O3, its related precursors, and meteorological parameters during the 2004 ICARTT study, J. Geophys. Res., 112, D12S14, doi:10.1029/2006JD007715, 2007

Yu, S., Mathur, R., Sarwar, G., Kang, D., Tong, D., Pouliot, G., and Pleim, J.: Eta-CMAQ air quality forecasts for O3 and related species using three different photochemical mechanisms (CB4, CB05, SAPRC-99): comparisons with measurements during the 2004 ICARTT study, Atmos. Chem. Phys., 10, 3001– 3025, doi:10.5194/acp-10-3001-2010, 2010.

Zhang, J., Rao, S.T., 1999. The role of vertical mixing in the temporal evolution of ground-level ozone concentrations. Journal of Applied Meteorology, 38, 1674-1691

Zyryanov D., G. Foret, M. Eremenko, M. Beekmann, J-P Cammas, M.D'Isidoro, H. Elbern, J. Flemming, E. Friese, I. Kioutsioutkis, A. Maurizi, D.Melas, F. Meleux, L. Menut, P. Moinat, V-H Peuch, A. Poupkou, M. Razinger, M. Schultz, O. Stein, A. M. Suttie, A. Valdebenito, C. Zerefos, G. Dufour, G. Bergametti and J-M. Flaud, 2012, 3D evaluation of tropospheric ozone simulations by an ensemble of regional Chemistry Transport Model, Atmospheric Chemistry and Physics, 12, 3219-3240.

Tables

Table 1 Airport domains and number of hourly flights during 2006 for each variable. The airports selected for analyses are highlighted in bold

Domain	Airports	IATA Code	Num. of Avail. flights	ozone	CO	T	RH	WS	WD
West Cast	**Portland**	**KPDX**	**142**	**126**	**135**	**142**	**142**	**142**	**142**
	Vancouver	CYVR	72	62	65	72	72	72	72
Atlanta	**Atlanta**	**KATL**	**142**	**126**	**129**	**142**	**141**	**142**	**142**
	Charlotte	KCLT	2	2	2	2	2	2	2
East Coast	Boston	KBOS	30	27	26	30	30	30	30
	Chicago	KORD	4	4	4	4	4	4	4
	Montreal	CYUL	2	2	2	2	2	2	2
	New York	KJFK	15	10	15	15	15	15	15
	Philadelphia	**KPHL**	**110**	**102**	**102**	**109**	**109**	**110**	**110**
	Toronto	CYYZ	90	72	72	89	89	89	89
	Washington	KIAD	62	28	54	61	61	62	62
Dallas	**Dallas**	**KDFW**	**124**	**124**	**114**	**121**	**124**	**124**	**124**
Central Europe	**Frankfurt**	**EDDF**	**1214**	**1088**	**1134**	**1134**	**1135**	**1135**	**1026**
	Munchen	EDDM	6	4	6	6	6	6	6
	Vienna	LOWW	374	291	374	360	374	374	249

Table 2. Participating models and features

Met	CTM	Resolution (km)	Vertical (bottom-top)	Emission	BC
			North America		
GEM	AURAMS	15x15	28 (14 in the first 2 km)	Standard[b]	Climatology
MM5	DEHM	50x50	29 (100 hPa)	Global emission database/EMEP[d]	Estimated from hemispheric domain
WRF	CMAQ	12x12	34 (25 m to 50 hPa)	Standard	Standard
WRF	CAMx	12	23 from 30 m	Standard	standard
Cosmo-CLM (CCLM)	CMAQ	24x24	30 (60 m to 100 hPa)	Standard[a]	Standard
			Europe		
MM5	DEHM	50x50	29 (100 hPa)	Global emission database/EMEP[d]	Estimated from hemispheric domain
ECMWF	SILAM	24	9 (10 km)	Standard	Standard
MM5	CHIMERE	25	9 (20 m to 500 hPa)	Standard	Standard, MEGAN
ECMWF	LOTOS-EUROS	25	4	Standard[a]	Standard
WRF	CMAQ	18	34 (20 m to 50 hPa)	Standard[a]	Standard
MM5	CAMx	15	23 (30 m to 12 km)	Standard	Standard
WRF	WRF-Chem1,2	22.5	35 (16 m to 50 hPa)	Supplied by WRF/Chem (constant background values)	Standard
Cosmo-CLM (CCLM)	CMAQ	24x24	30 (36 m to 100 hPa)	Standard[a]	Standard
MM5	Polyphemus	24	9 (up to 1200 m)	Standard[a,c]	Standard

[a] Standard anthropogenic emission and biogenic emission derived from meteorology (temperature and solar radiation) and land use distribution implemented in the meteorological driver (Guenther et al., 1994; Simpson et al., 1995).
[b] Standard anthropogenic inventory but independent emissions processing, exclusion of wildfires, and different version of BEIS (v3.09) used
[c] Emissions Includes: Biomass burning; Biogenic organic compounds of SOA:a-pinene, limonene, sesquiterpene, hydrophilic isoprene.
[d] Global: IPCC RCP 3-PD Lamarque et al. (2010); Bond et al. (2007); Smith et al. (2001); Ships: Corbett and Fischbeck (1997); GEIA natural emissions (Graedel et al., 1993); Wildfires as in Schultz et al. (2008). Europe: EMEP (Vestreng and Støren, 2000)

Figures

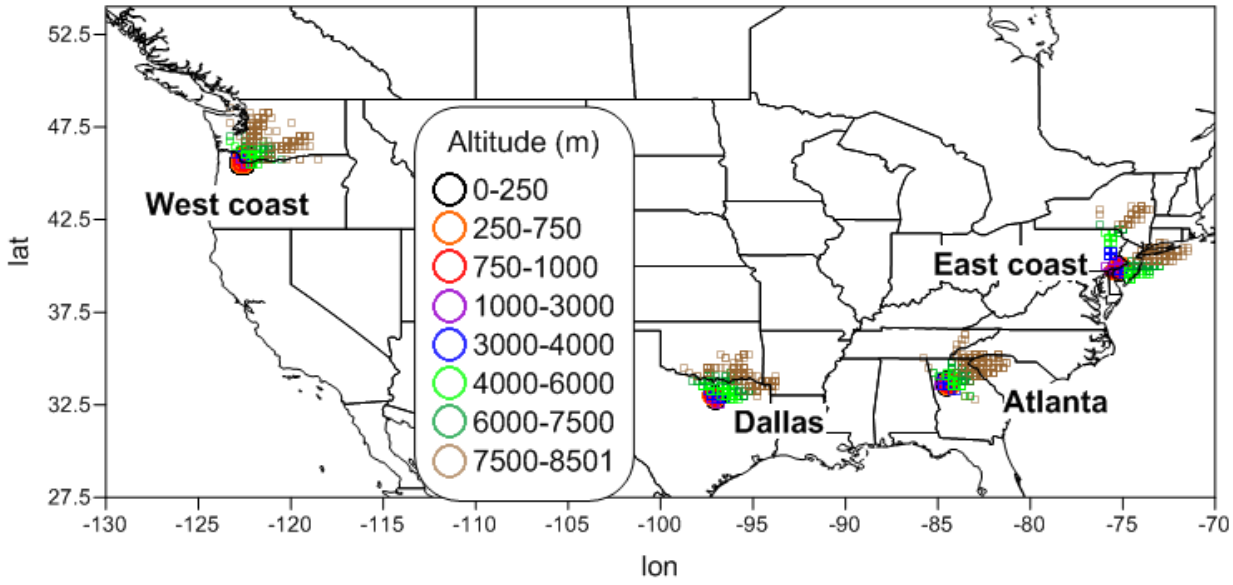

a)

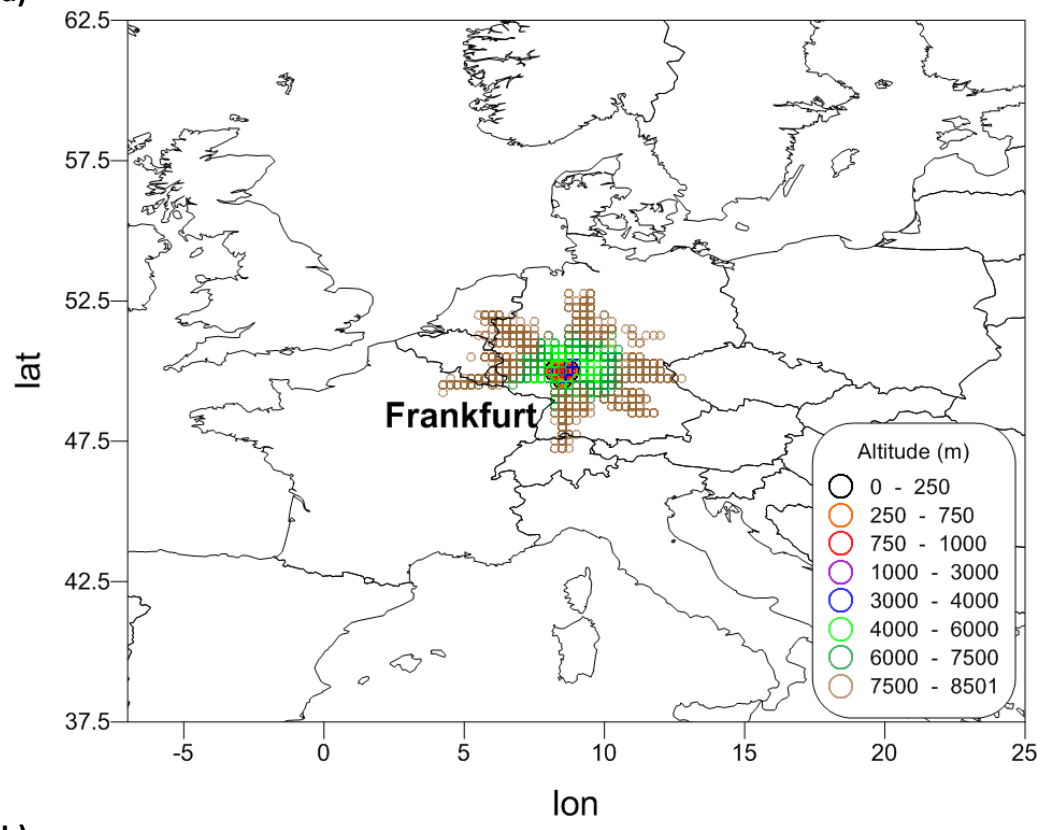

b)

Figure 1. Flight trajectories by height for the selected airports in **a)** North America and **b)** Europe.

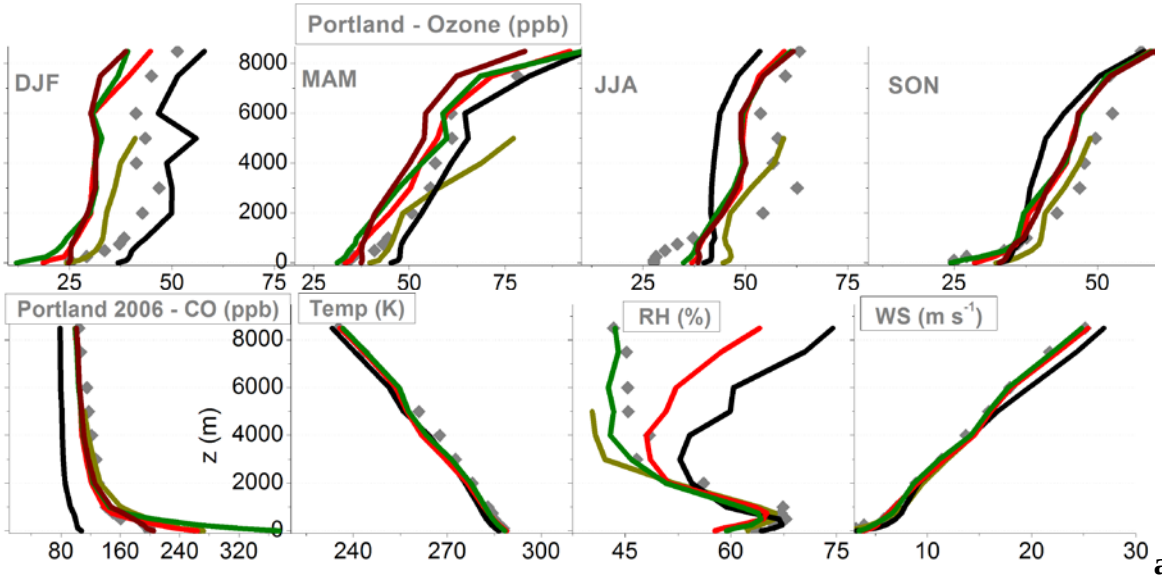
Portland - Ozone (ppb)
DJF
MAM
JJA
SON
Portland 2006 - CO (ppb)
Temp (K)
RH (%)
WS (m s-1)
z (m)

a)

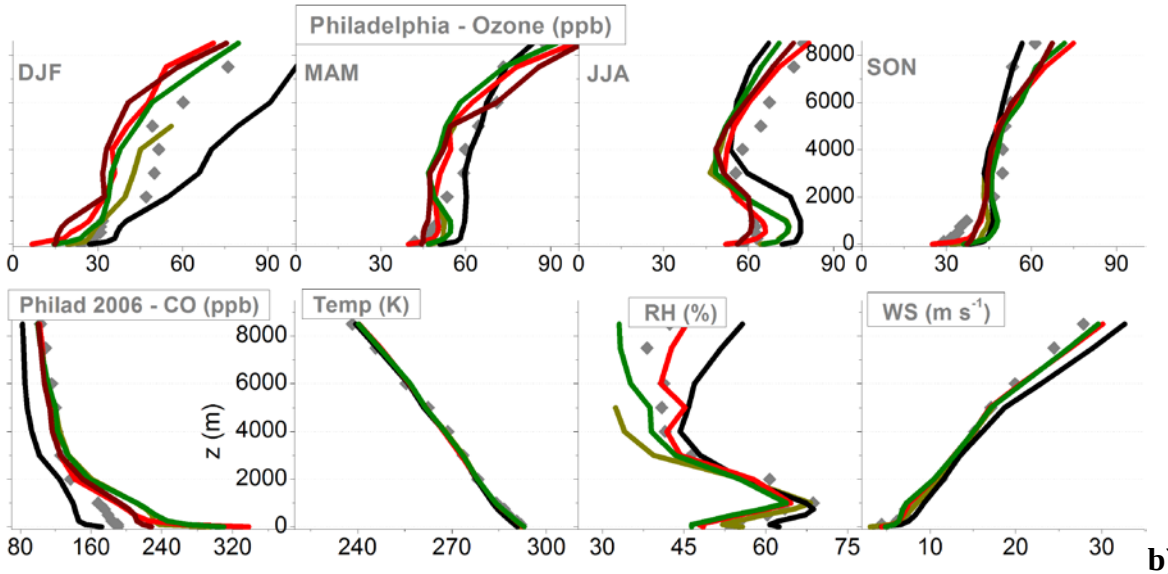
Philadelphia - Ozone (ppb)
DJF
MAM
JJA
SON
Philad 2006 - CO (ppb)
Temp (K)
RH (%)
WS (m s-1)
z (m)

b)

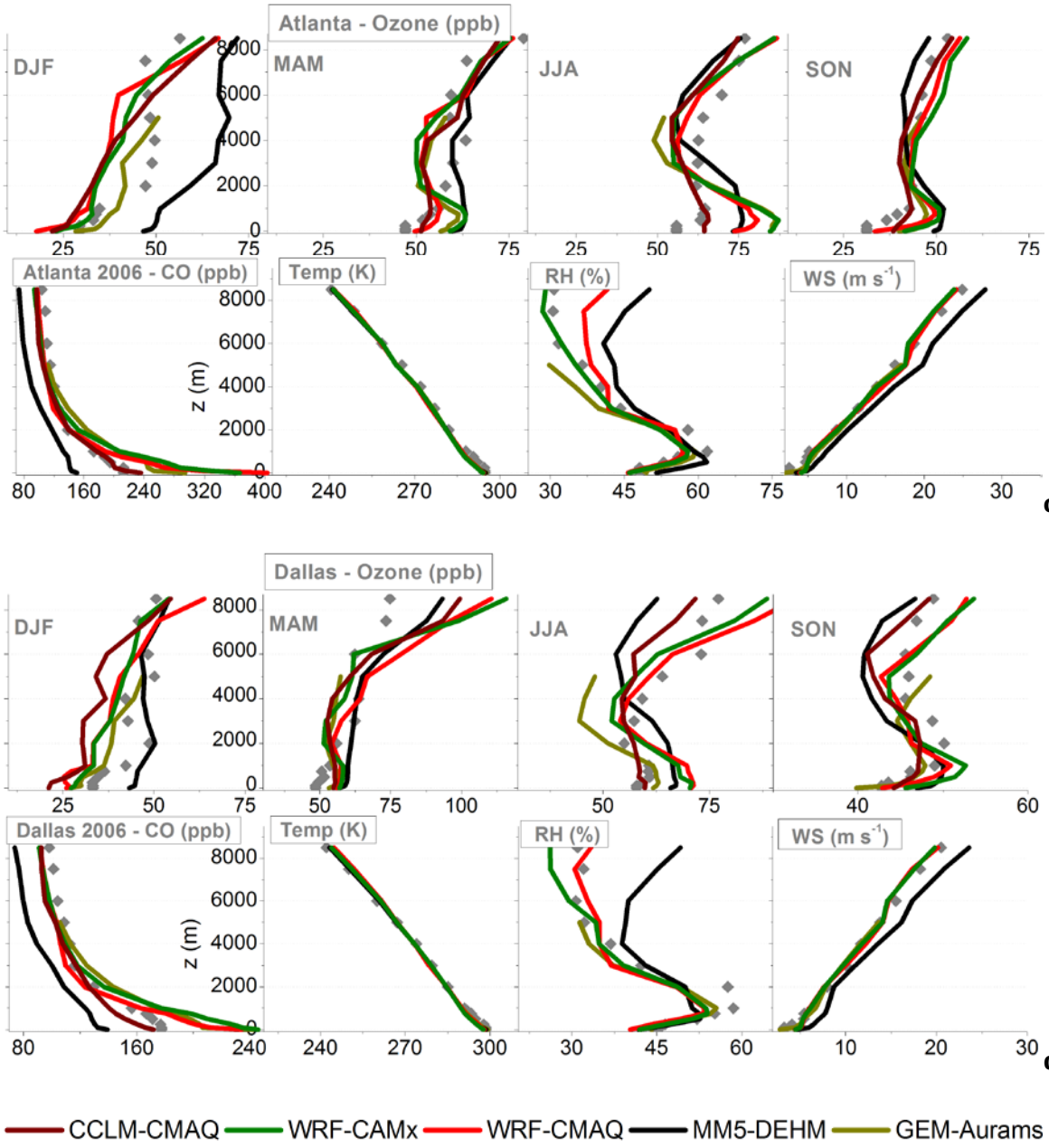
Atlanta - Ozone (ppb)
DJF
MAM
JJA
SON
Atlanta 2006 - CO (ppb)
Temp (K)
RH (%)
WS (m s-1)
z (m)
c)
Dallas - Ozone (ppb)
Dallas 2006 - CO (ppb)
d)
CCLM-CMAQ
WRF-CAMx
WRF-CMAQ
MM5-DEHM
GEM-Aurams

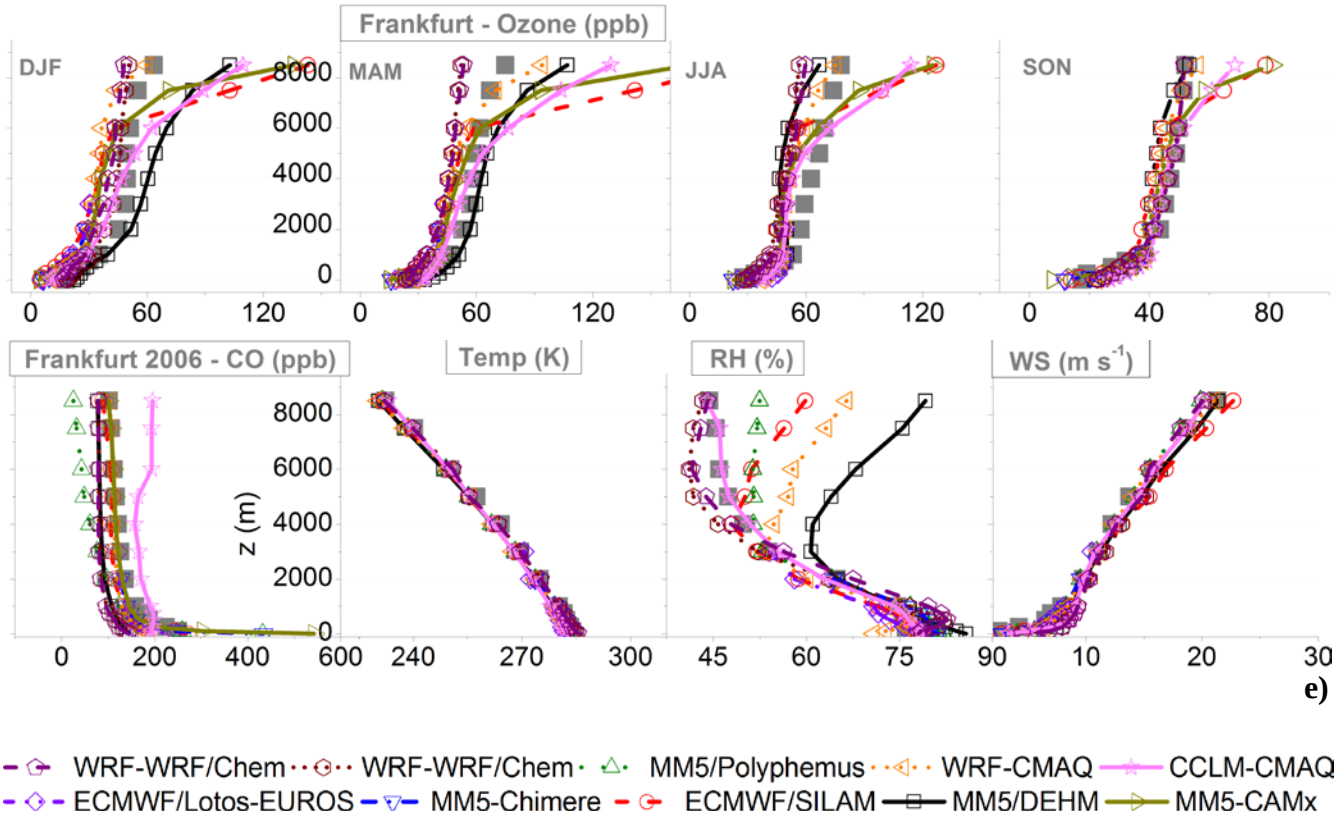

Figure 2. Seasonal averaged mean profiles of ozone (top rows) and annual averaged mean profiles of CO, temperature, relative humidity (RH) and wind speed (WS) (year 2006) for **a)** Portland, **b)** Philadelphia, **c)** Atlanta, **d)** Dallas, and **e)** Frankfurt. The grey symbols are the observations.

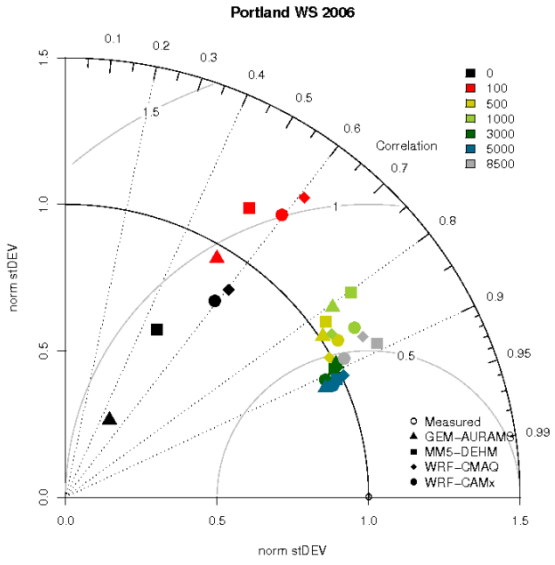
Portland WS 2006
Correlation
norm stDEV
0
100
500
1000
3000
5000
8500
Measured
GEM-AURAMS
MM5-DEHM
WRF-CMAQ
WRF-CAMx

a

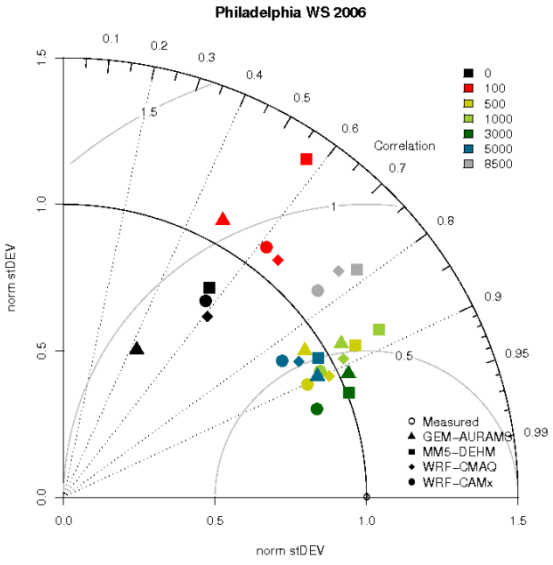
Philadelphia WS 2006
Correlation
norm stDEV
0
100
500
1000
3000
5000
8500
Measured
GEM-AURAMS
MM5-DEHM
WRF-CMAQ
WRF-CAMx

b

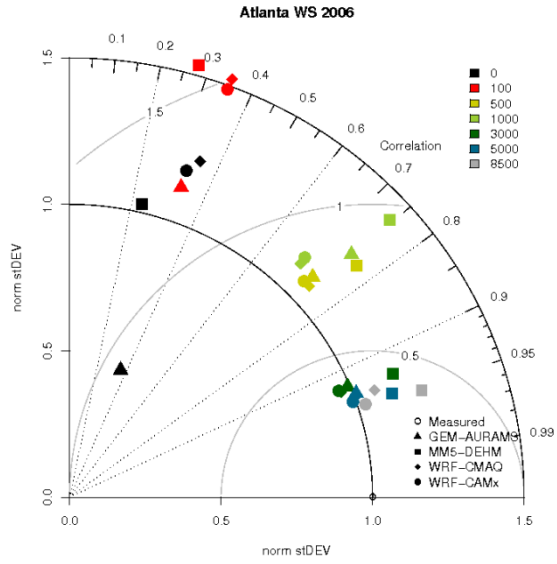
Atlanta WS 2006
Correlation
norm stDEV
0
100
500
1000
3000
5000
8500
Measured
GEM-AURAMS
MM5-DEHM
WRF-CMAQ
WRF-CAMx

c

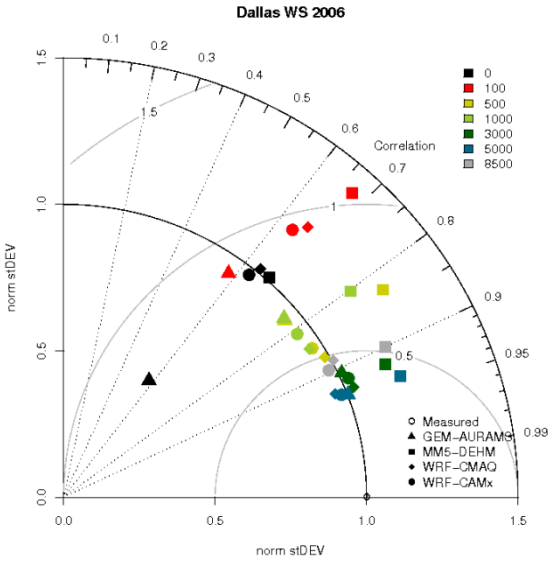
Dallas WS 2006
Correlation
norm stDEV
0
100
500
1000
3000
5000
8500
Measured
GEM-AURAMS
MM5-DEHM
WRF-CMAQ
WRF-CAMx

d

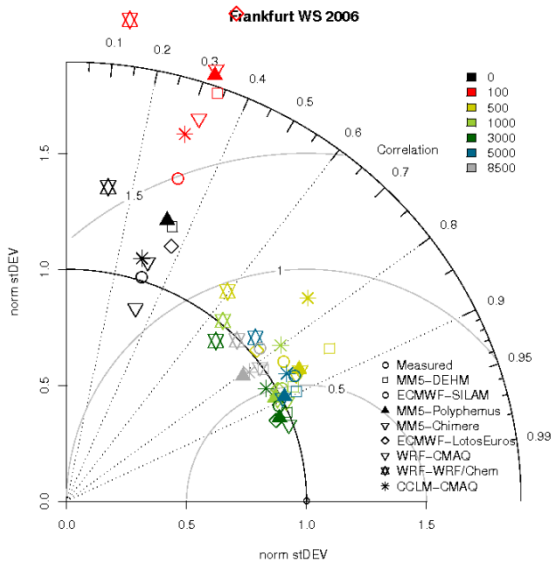

e

Figure 3 - Taylor diagrams for wind speed at a) Portland; b) Philadelphia; c) Atlanta; d) Dallas; e) Frankfurt. Height by colours, model by symbols

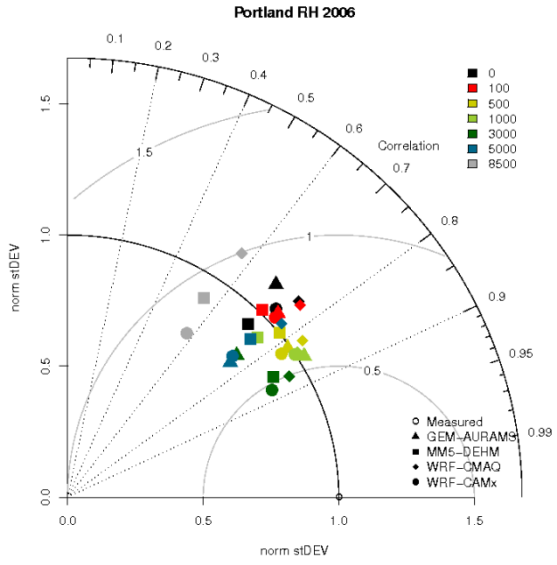
Portland RH 2006
Correlation
norm stDEV
0
100
500
1000
3000
5000
8500
Measured
GEM–AURAMS
MM5–DEHM
WRF–CMAQ
WRF–CAMx

a

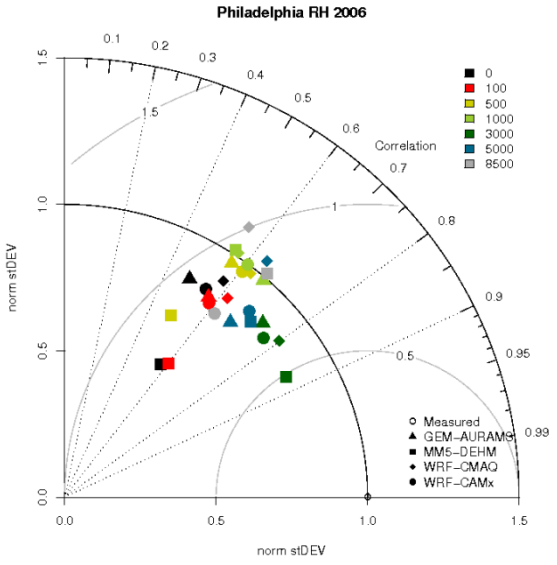
Philadelphia RH 2006
Correlation
norm stDEV
0
100
500
1000
3000
5000
8500
Measured
GEM–AURAMS
MM5–DEHM
WRF–CMAQ
WRF–CAMx

b

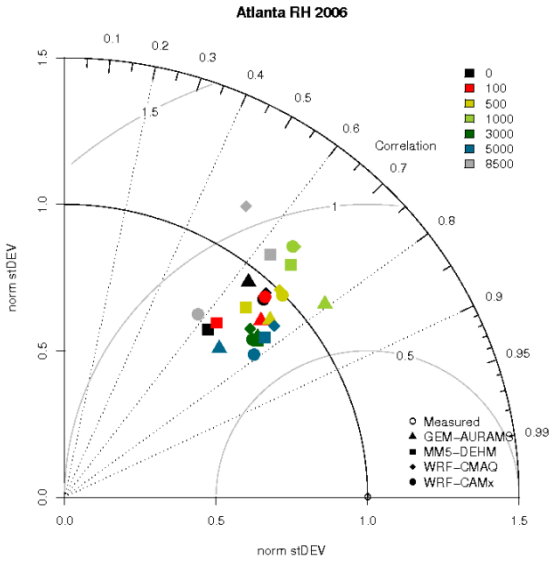
Atlanta RH 2006
Correlation
norm stDEV
0
100
500
1000
3000
5000
8500
Measured
GEM–AURAMS
MM5–DEHM
WRF–CMAQ
WRF–CAMx

c

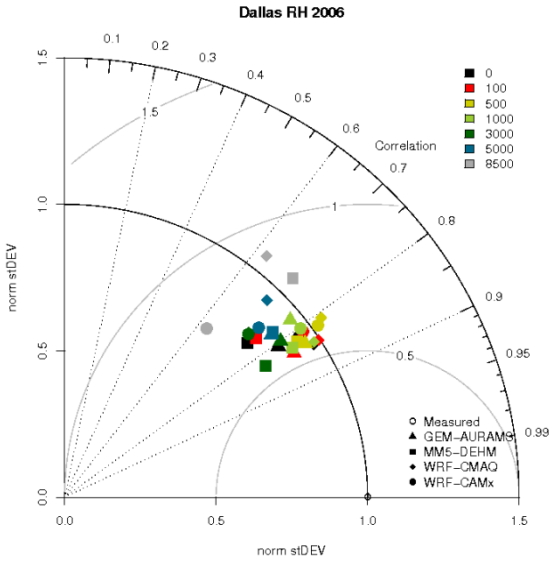
Dallas RH 2006
Correlation
norm stDEV
0
100
500
1000
3000
5000
8500
Measured
GEM–AURAMS
MM5–DEHM
WRF–CMAQ
WRF–CAMx

d

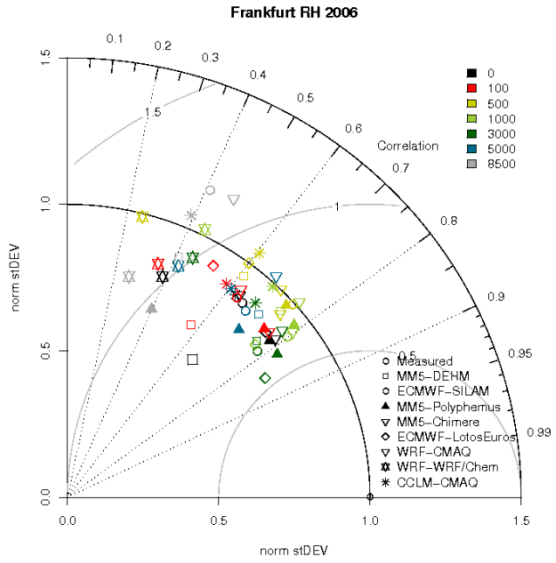

e

Figure 4 Taylor diagrams for relative humidity at **a)** Portland; **b)** Philadelphia; **c)** Atlanta; **d)** Dallas; **e)** Frankfurt. Height by colours, model by symbols

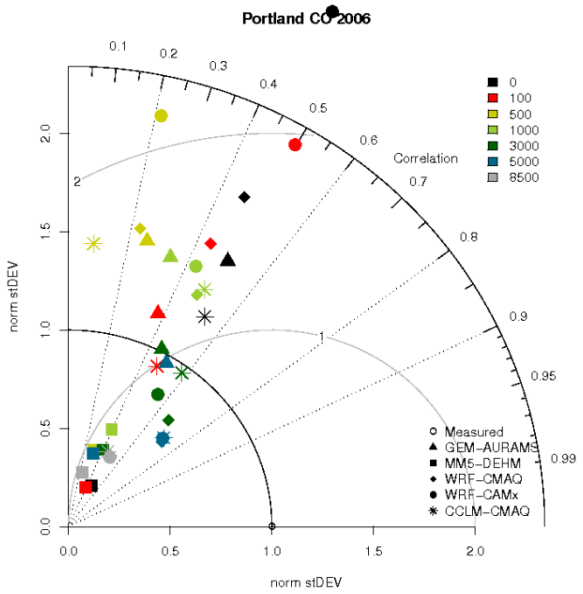
Portland CO 2006
norm stDEV
Correlation
0
100
500
1000
3000
5000
8500
Measured
GEM–AURAMS
MM5–DEHM
WRF–CMAQ
WRF–CAMx
CCLM–CMAQ

a

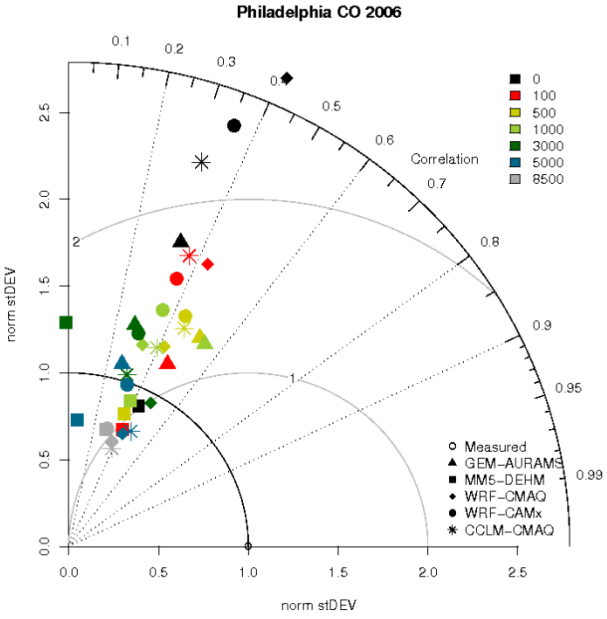
Philadelphia CO 2006
norm stDEV
Correlation
0
100
500
1000
3000
5000
8500
Measured
GEM–AURAMS
MM5–DEHM
WRF–CMAQ
WRF–CAMx
CCLM–CMAQ

b

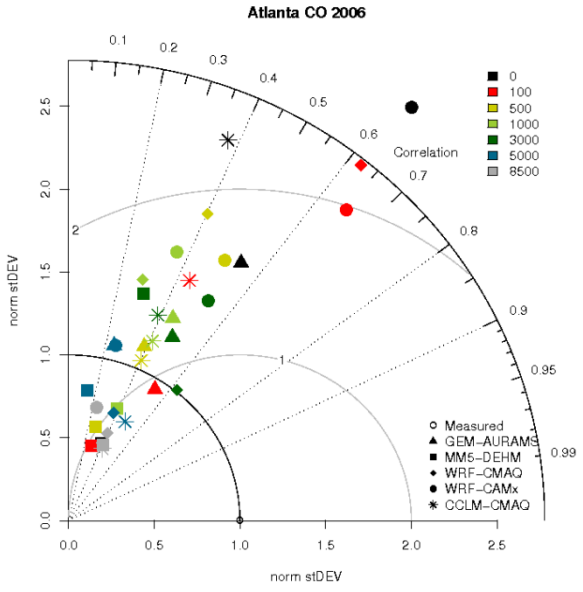
Atlanta CO 2006
norm stDEV
Correlation
0
100
500
1000
3000
5000
8500
Measured
GEM–AURAMS
MM5–DEHM
WRF–CMAQ
WRF–CAMx
CCLM–CMAQ

c

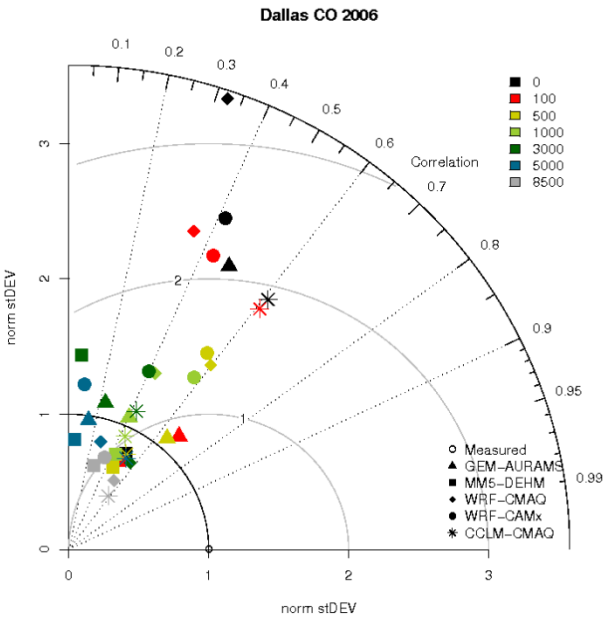
Dallas CO 2006
norm stDEV
Correlation
0
100
500
1000
3000
5000
8500
Measured
GEM–AURAMS
MM5–DEHM
WRF–CMAQ
WRF–CAMx
CCLM–CMAQ

d

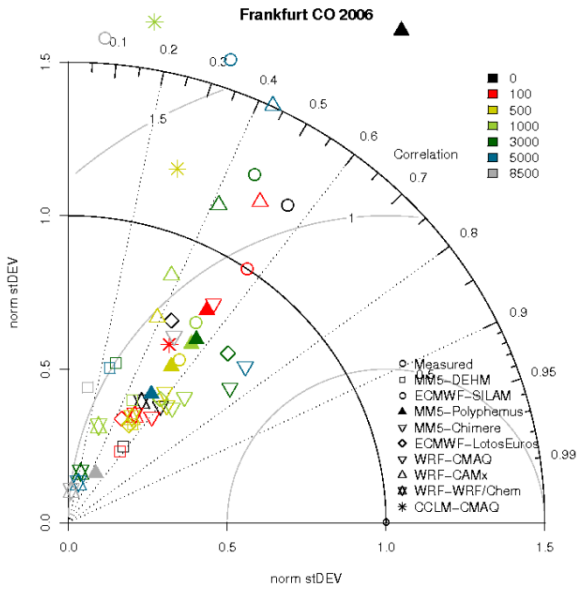

e

Figure 5a Taylor diagrams for CO at **a)** Portland; **b)** Philadelphia; **c)** Atlanta; **d)** Dallas; **e)** Frankfurt. Height by colours, model by symbols

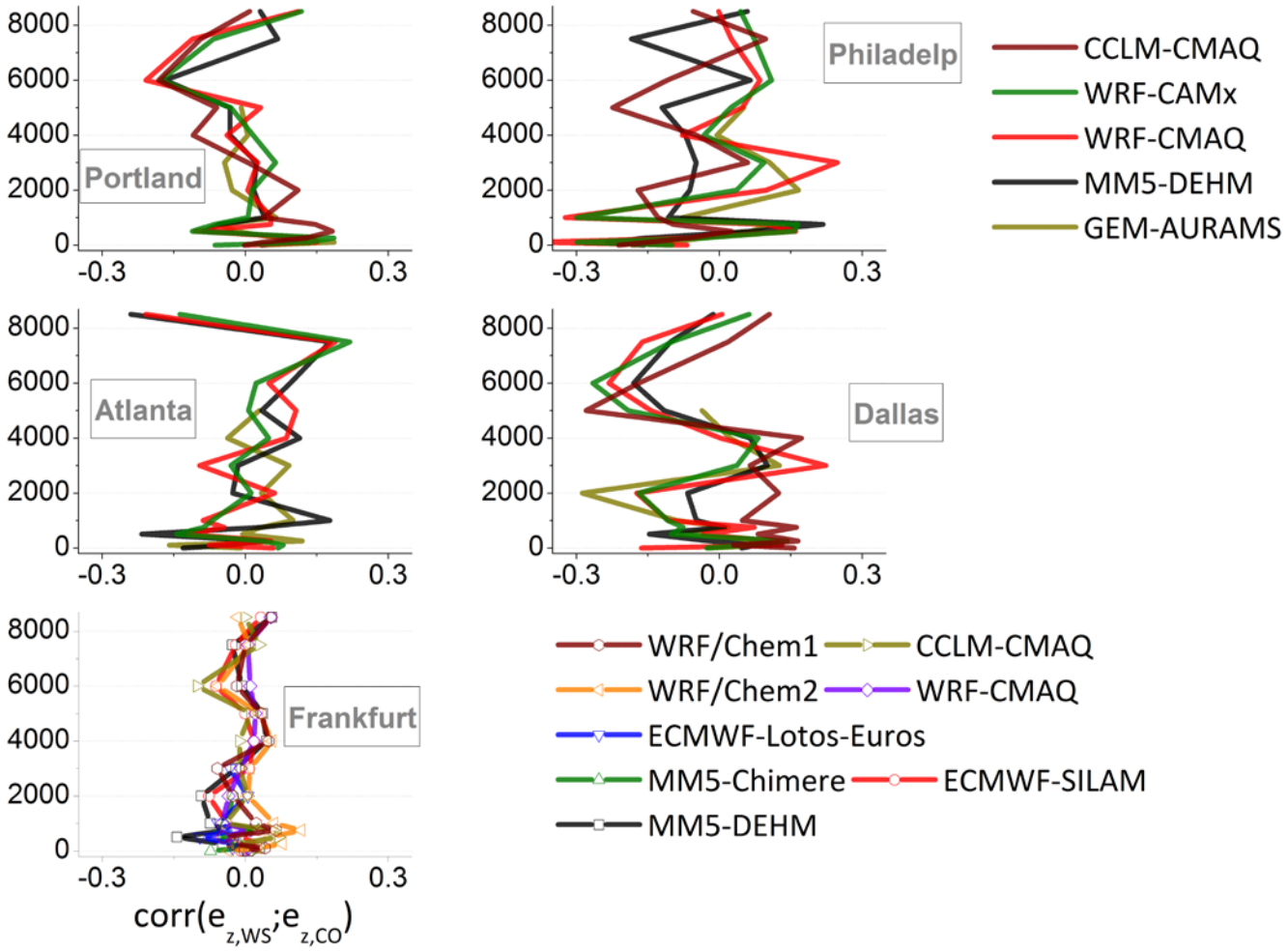

Figure 5b. Profiles of correlation between the WS and CO errors for the airports of Portland, Philadelphia (first row), Atlanta, Dallas (middle row), and Frankfurt (lower panel).

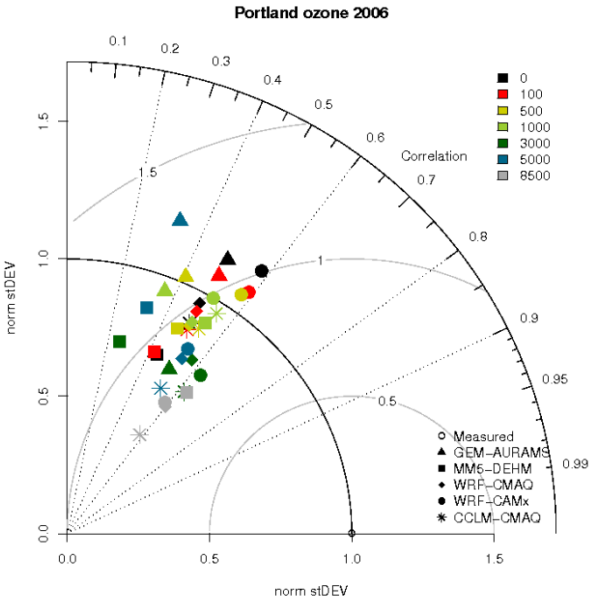
Portland ozone 2006
Correlation
norm stDEV
0
100
500
1000
3000
5000
8500
Measured
GEM–AURAMS
MM5–DEHM
WRF–CMAQ
WRF–CAMx
CCLM–CMAQ

a

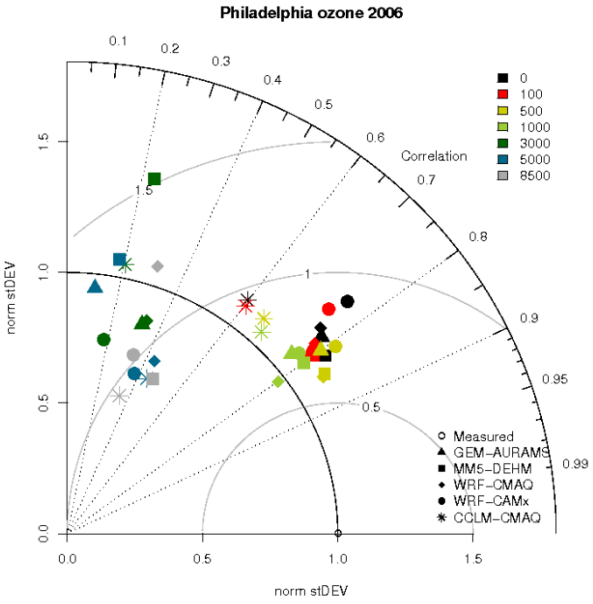
Philadelphia ozone 2006
Correlation
norm stDEV
0
100
500
1000
3000
5000
8500
Measured
GEM–AURAMS
MM5–DEHM
WRF–CMAQ
WRF–CAMx
CCLM–CMAQ

b

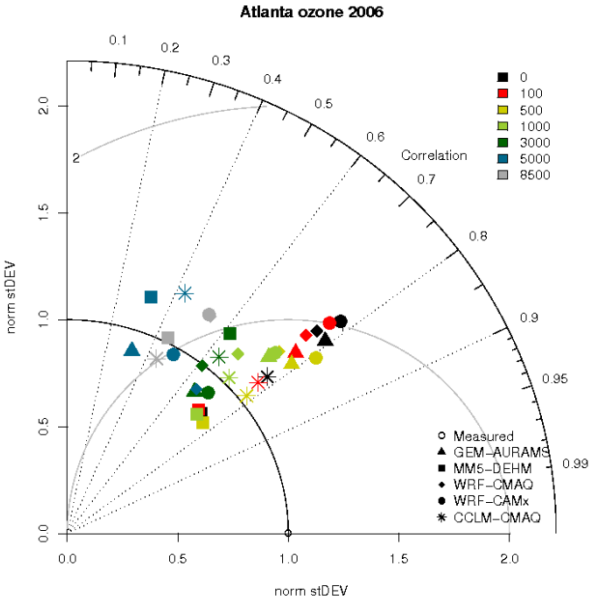
Atlanta ozone 2006
Correlation
norm stDEV
0
100
500
1000
3000
5000
8500
Measured
GEM–AURAMS
MM5–DEHM
WRF–CMAQ
WRF–CAMx
CCLM–CMAQ

c

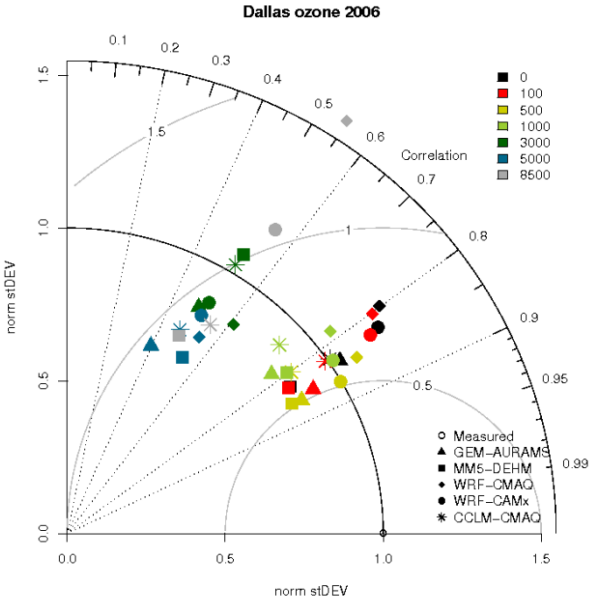
Dallas ozone 2006
Correlation
norm stDEV
0
100
500
1000
3000
5000
8500
Measured
GEM–AURAMS
MM5–DEHM
WRF–CMAQ
WRF–CAMx
CCLM–CMAQ

d

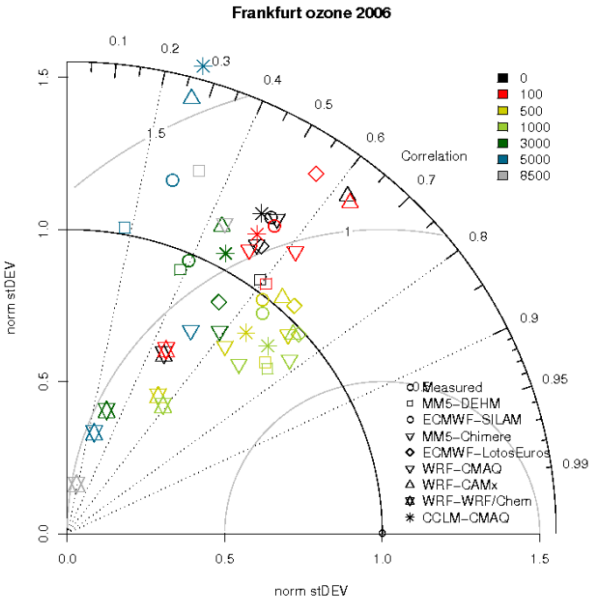

e

Figure 6 Taylor diagrams for ozone at **a)** Portland; **b)** Philadelphia; **c)** Atlanta; **d)** Dallas; **e)** Frankfurt. Height by colours, model by symbols

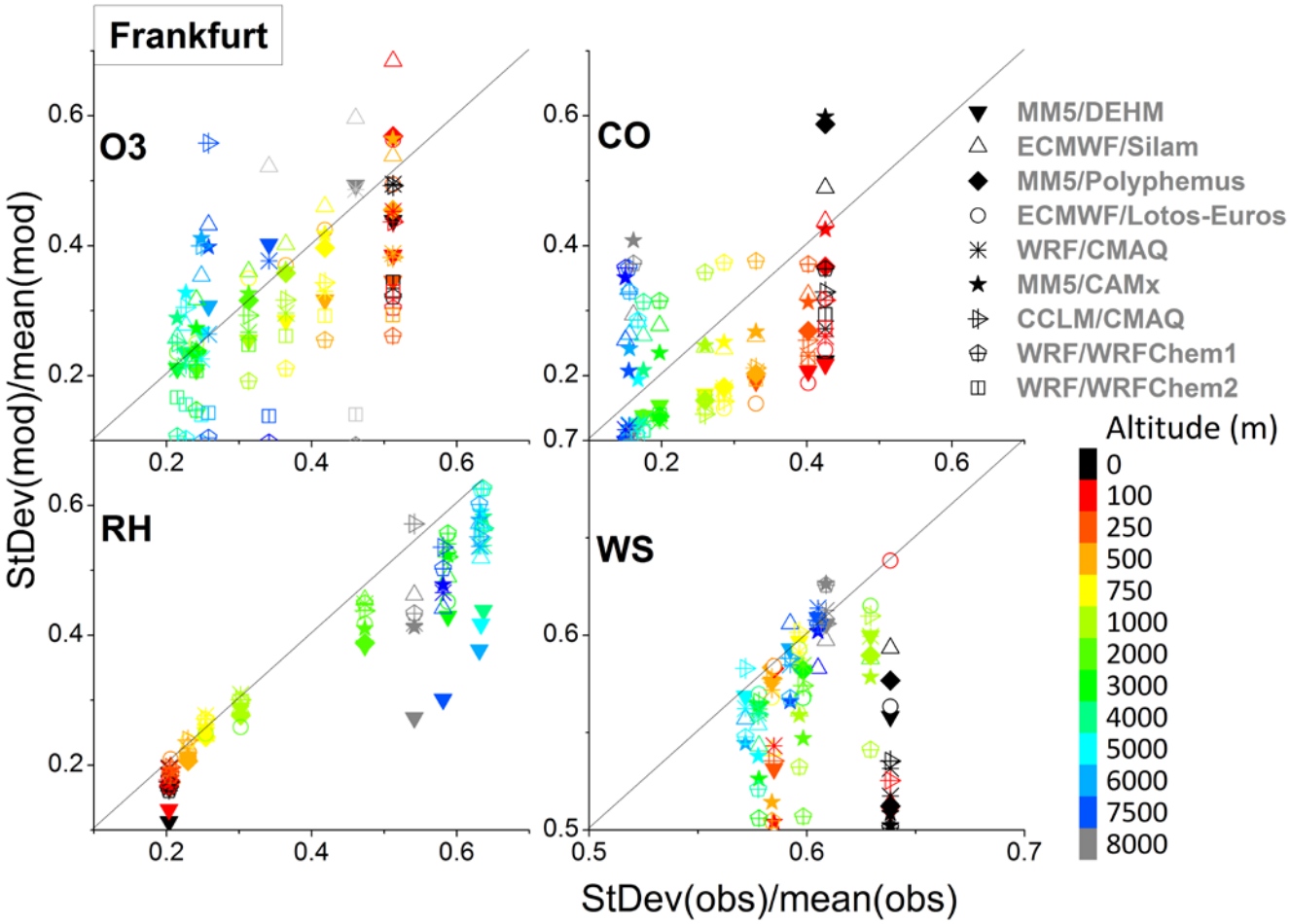

Figure 7. Modelled (vertical axis) versus observed (horizontal axis) coefficients of variation for Frankfurt (year 2006) for (clockwise from top-left): ozone, CO, RH, and WS. The straight line is the perfect agreement. Height by colours, model by symbols.

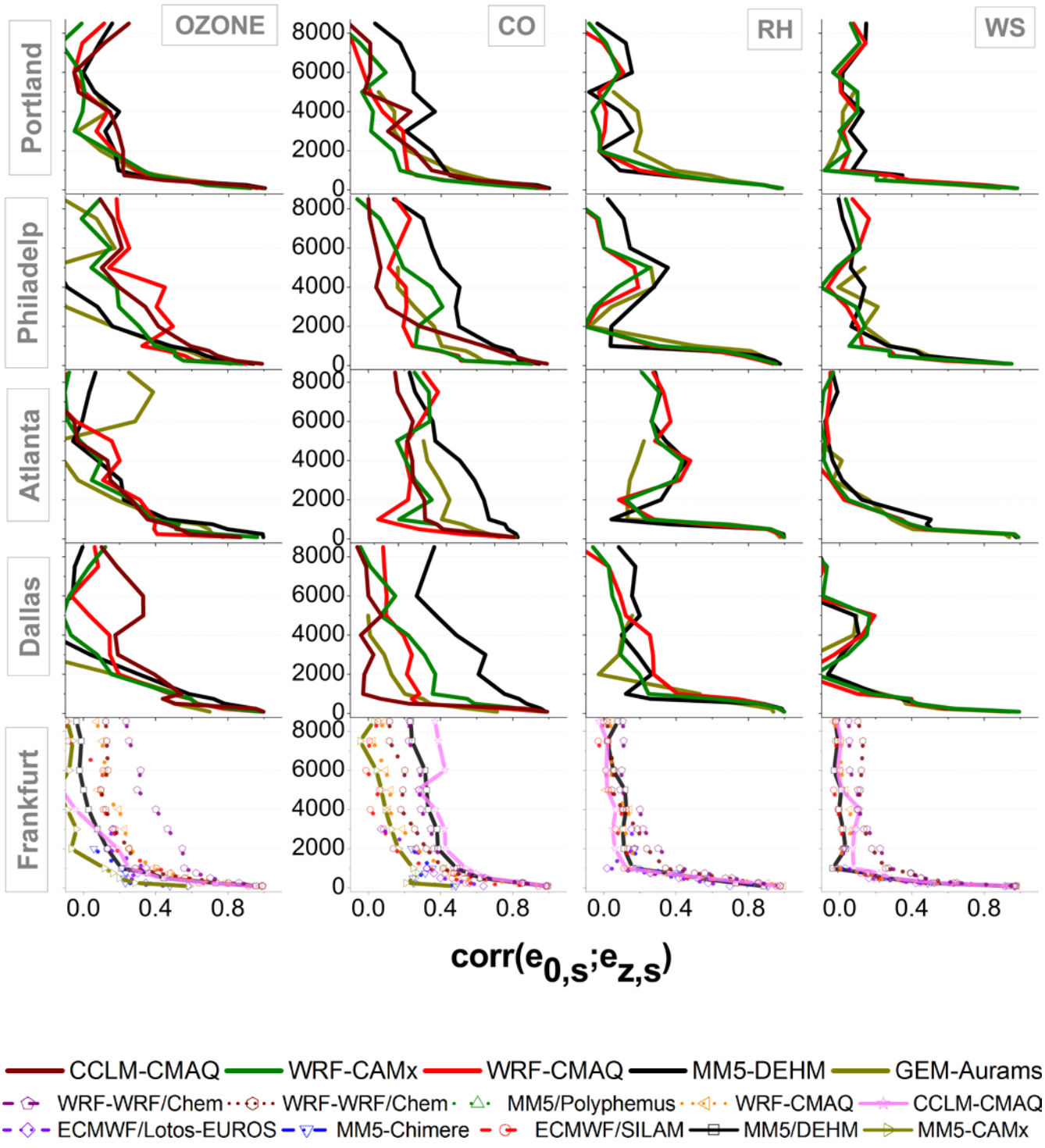

Figure 8. Correlation coefficient between the Fractional Difference (FD) at any height and the FD at the ground (z=0) for ozone, CO, RH, and WS (columns) and for the airports of Portland, Philadelphia, Atlanta, Dallas, and Frankfurt (rows) (year 2006). The first line of the legend refers to the NA models, while the other two lines to Frankfurt.

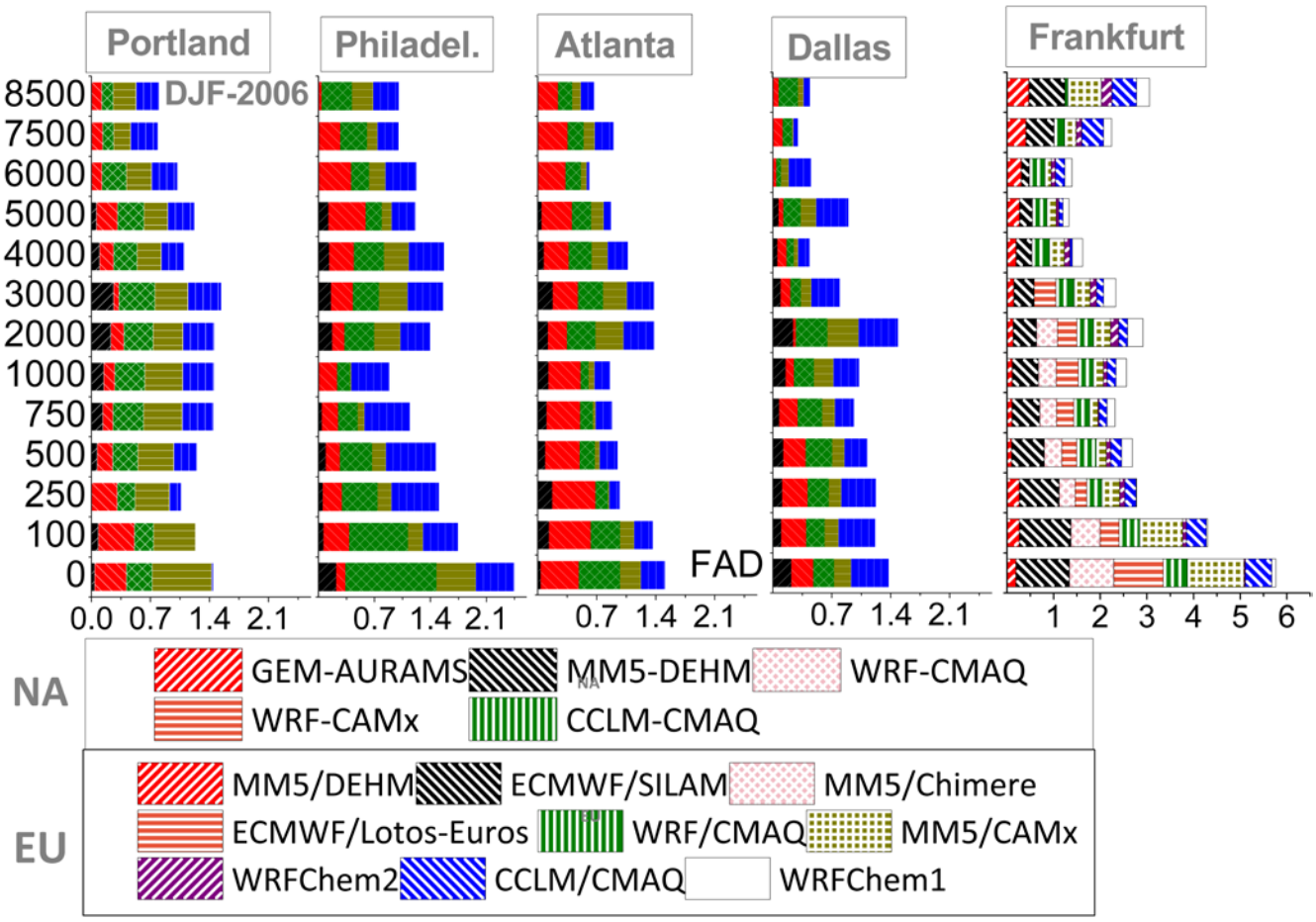

Figure 9 Cumulative Fractional Absolute Difference (FAD) of modelled ozone for the months of December, January, and February 2006.

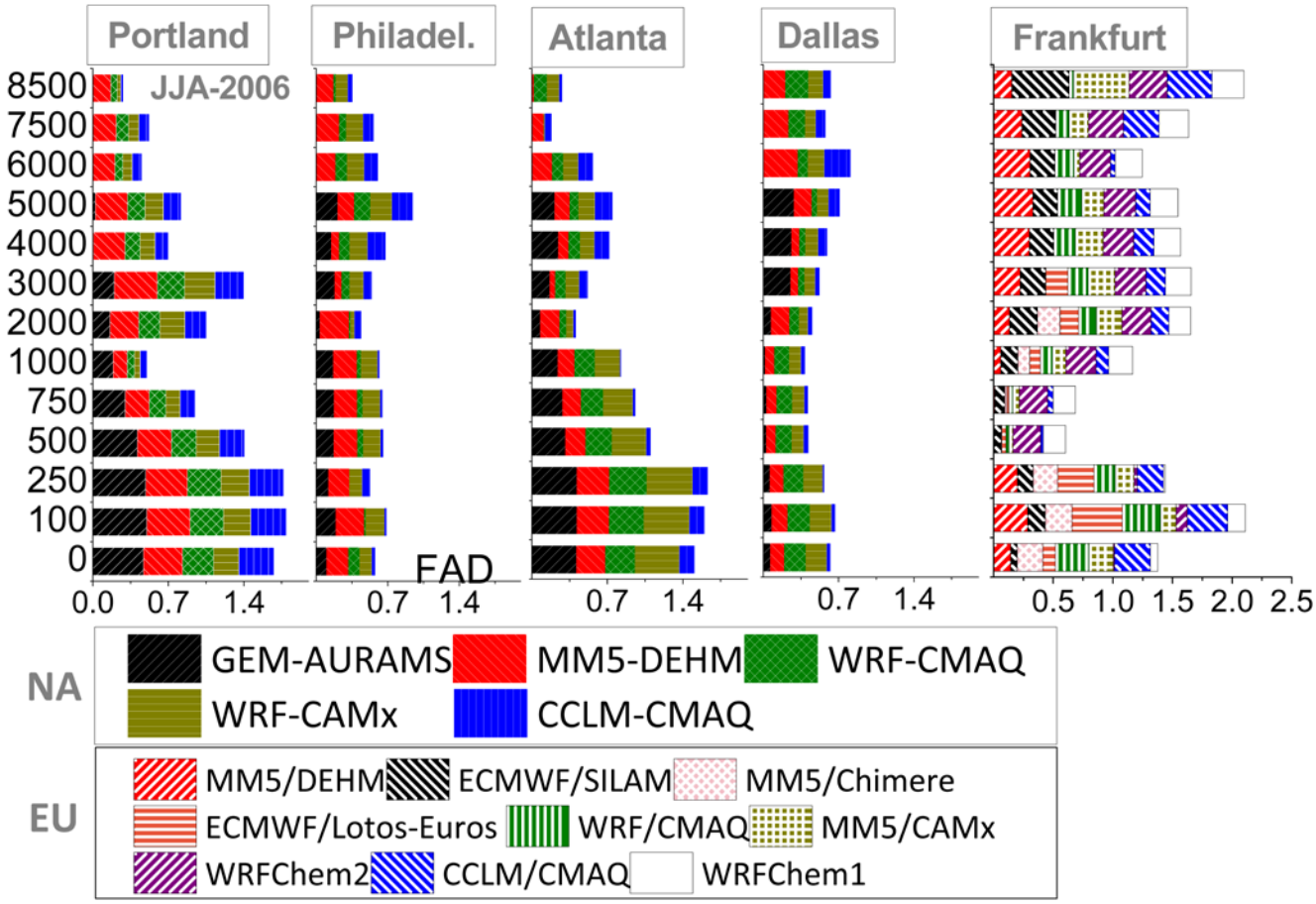

Figure 10. Cumulative Fractional Absolute Difference (FAD) of modelled ozone for the months of June, July, and August 2006.

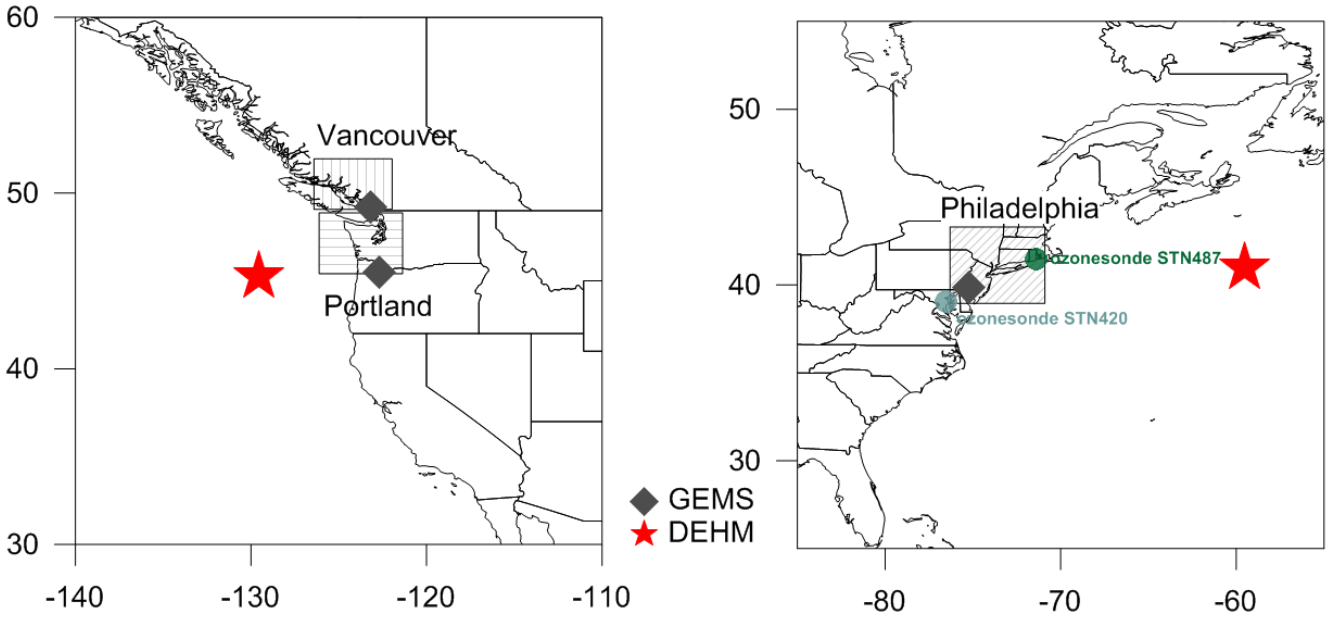

Figure 11. Positions where BCs data are provided for GEMS and DEHM (position for AURAMS is the same as for GEMS). For the East Coast of NA the locations of two ozonesondes used in the analysis are also shown. The shaded areas indicate the extension of the domain around the airport

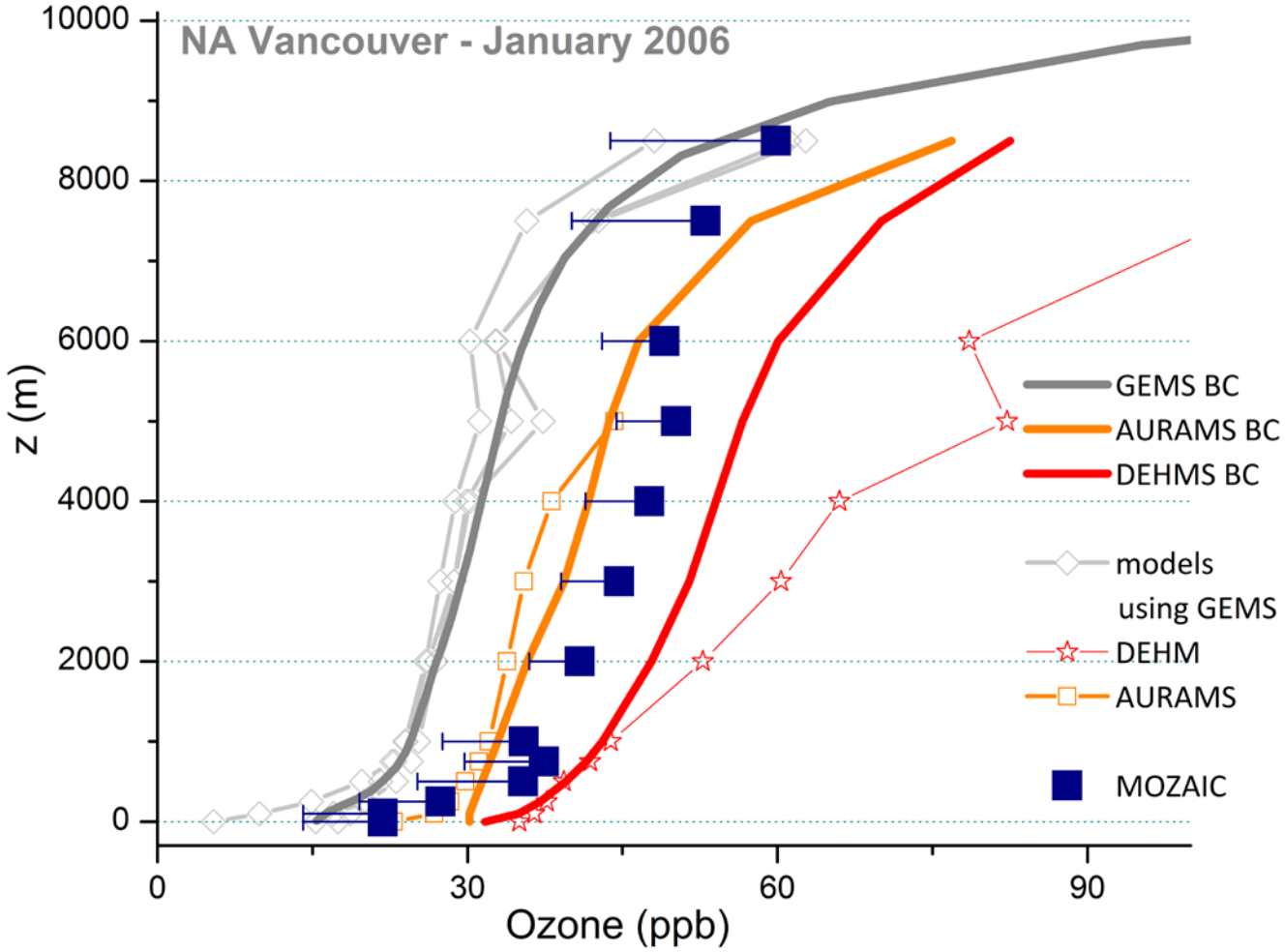

Figure 12. Monthly averaged vertical profiles of ozone for Vancouver, January 2006: BCs providers (thick lines), AQ model outputs (thin lines), MOZAIC (filled squares). The horizontal lines by the measurements are the standard deviations (symmetric about the mean point, thus only the left portion is shown).

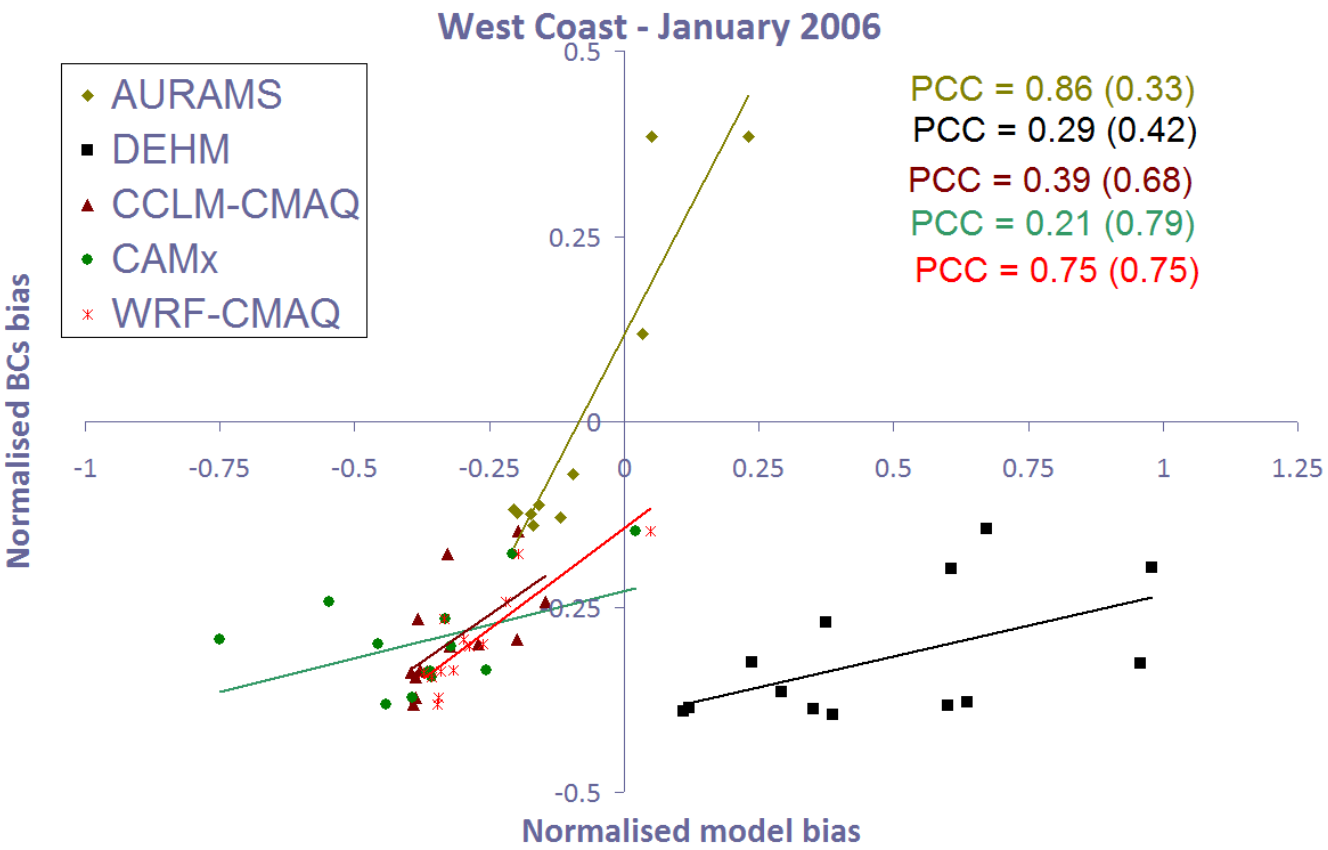

Figure 13 Normalised modelled vs. BCs bias with respect to MOZAIC for the month of January 2006 for the Portland airport. The two CMAQ instances and CAMx use the same BCs. The continuous lines are derived from the linear regression fit, with the squared correlation coefficients reported on the top right corner (color coded). In parenthesis are the squared coefficients obtained by correlating the bias excluding the data in the first 250m (i.e. by including data from 500 m to 8.5 km).

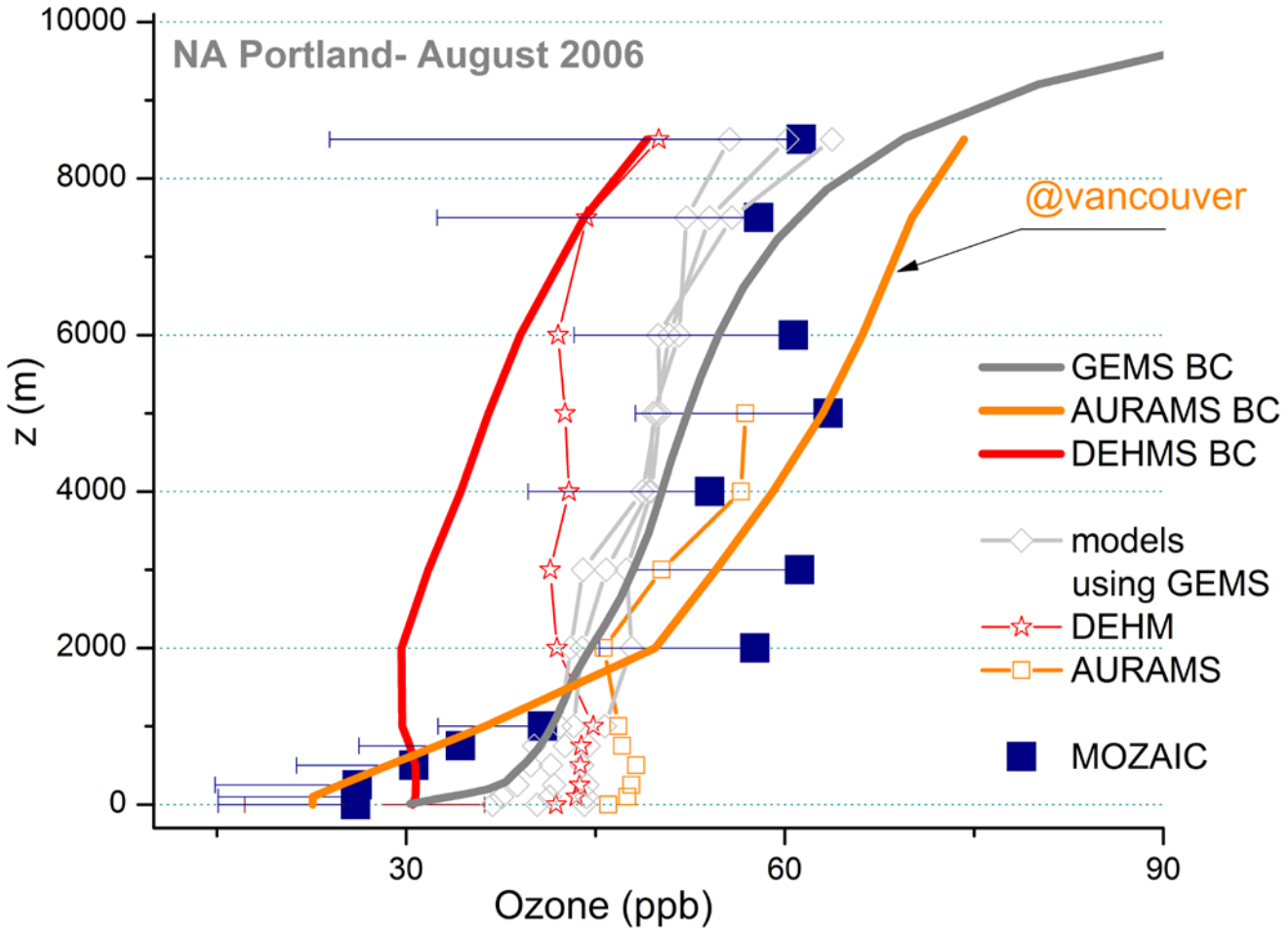

Figure 14. Monthly averaged vertical profiles of ozone for Portland, August 2006. The BC for the AURAMS model (thick orange line) was provided at Vancouver.

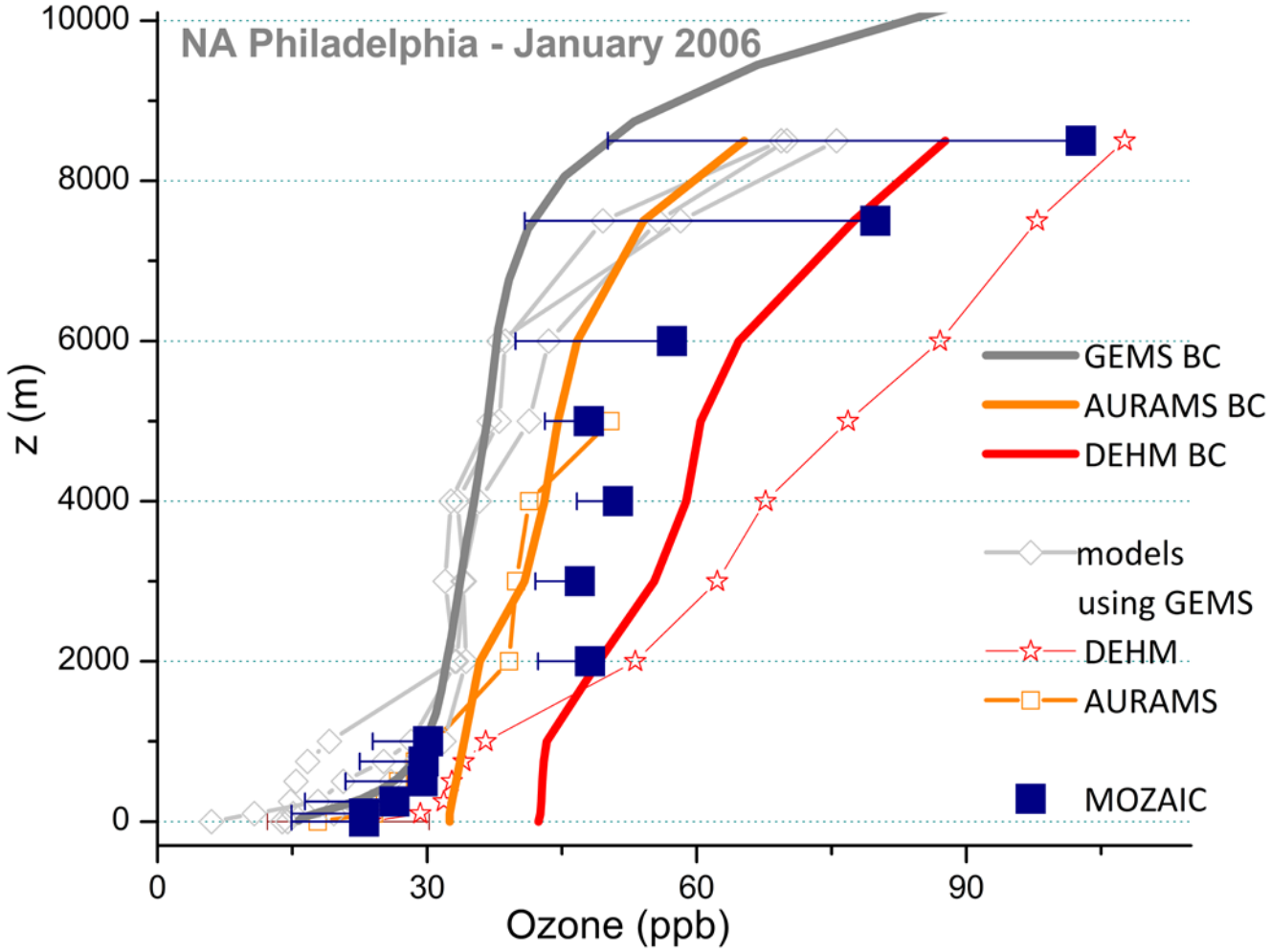

Figure 15 Monthly averaged vertical profiles of ozone for Philadelphia, January 2006.

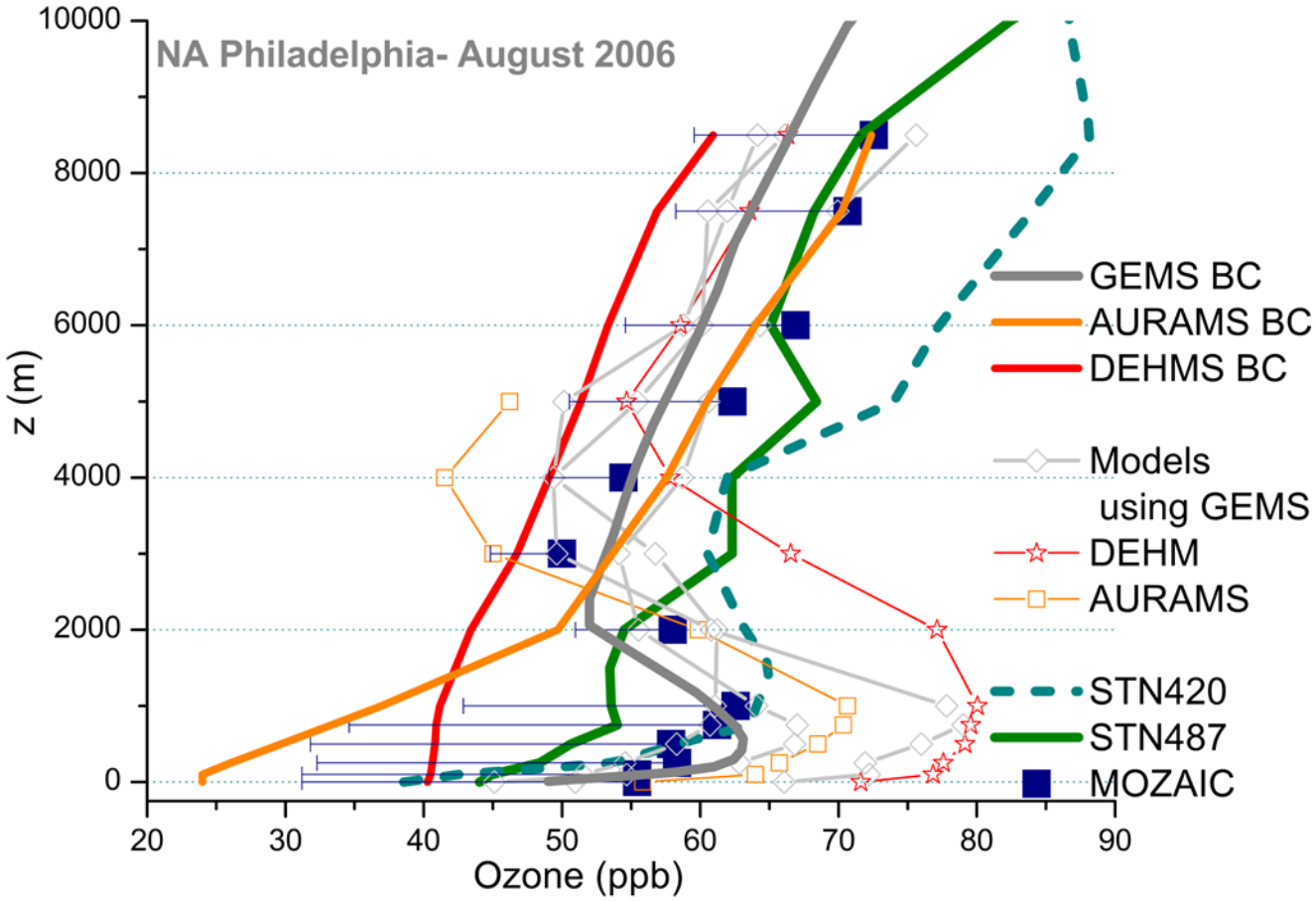

Figure 16 Monthly averaged vertical profiles of ozone for Philadelphia, August 2006. Monthly averaged ozonesonde profiles from two nearby rural locations (see Figure 11) are also reported.